Universitat de les
Illes Balears

Title: Evolution of movement strategies under competitive interactions

AUTHOR: Danis Kiziridis

Master's Thesis

Master's degree in Physics of Complex Systems

at the

UNIVERSITAT DE LES ILLES BALEARS

Academic year 2013 - 2014

UIB Master's Thesis Supervisor Emilio Hernández-García

UIB Master's Thesis Co-Supervisor Cristóbal López

Contents

1. Abstract

One of the proposed selective forces for the evolution of dispersal, the opposition between temporal and spatial variation, seems to accumulate considerable empirical and theoretical support: slower dispersers are selected in more heterogeneous environments, since colonizing other sites imposes higher risk of ending up on lower quality space; while faster dispersers are fitter in larger population fluctuations by escaping highly competitive sites and colonizing emptier, less competitive ones. While most of the theoretical models studying this opposition are based on the metapopulation framework, a test of the importance of this selective force under a different modeling scheme would be welcome. We adopt a model of point-like individuals in a resource homogeneous domain, where spatial variation arises in a self-organizing manner because of the neighborhood density dependence of the demographic rates. Initially, we distinguish two model demographic parameters which might affect temporal and spatial variation, and we organize numerical evolutionary experiments. We manage to replicate previous, pairwise species competitions' results of the model, where the superiority of slower dispersers was exhibited, at this time with the different approach of simulating population evolution under an eco-evolutionary setting. By experimenting and measuring spatial and temporal variation, as they were manipulated by the two demographic parameters, we observe the redirection of selection from one extreme of mobility to the other. Specifically, we find that increased competition intensity and competition-mediated death rates result in higher temporal in respect to spatial variation, which by their turn result to the selection of higher mobility. The incorporation of the modern scheme of eco-evolutionary feedback helped greatly in the explanation of the evolutionary outcomes. In conclusion, this study confirmed from a different modeling view, in which spatial and temporal variation were not imposed explicitly and externally, the importance of the opposition between temporal and spatial variation for the evolution of dispersal.

2. Introduction

2.1. Terminology of ecological movement

A search in the ecological literature reveals different terms for various aspects of the movement of biological organisms, and some basic information about their possible roots and their meaning might prove useful at the beginning. Some of the most popular terms are 'dispersal', 'foraging', and 'migration'. A main responsible of such a separateness seems to be the metapopulation conceptualization of the ecological systems, which categorizes space as habitat or non-habitat (Hawkes, 2009). Specifically, the ecological chessboard, according to this paradigm, consists of discrete 'oases' of appropriate habitat laid on an unfriendly 'desert'. The dynamics occur at two inter-linked levels: the population level, where each patch may host a population; and the metapopulation level where individuals leave their patches, move across the non-hostile terrain, and enter other patches. Dispersal, according to its traditional notion, refers to the movement of the offspring away from the parental neighborhood, principally to a different habitat patch. Foraging is used to describe small-scale search movements inside a patch. And migration is left for the seasonal movements between wintering and breeding sites.

While these definitions seem clear, it is recognized that, due to high variation across species, the non-discrete temporal nature of the organism life history, and the frequent inability of a clear delineation of a habitat patch, their definition becomes less strict and narrow (Hawkes, 2009). For example, the narrow meaning of dispersal has been expanded to incorporate any patch-to-patch trans-location. Still, though, after this expansion these terms step on valid grounds as long as there are borders, even blurred, between disciplines. For example, a behavioral biologist's focus probably would not be dispersal, but she/he would care about the foraging behavior of individuals around the nest; while a macroecologist would ignore the small-scale spatial patterns of individuals, focusing instead on how, for example, the abiotic environmental gradients in combination with dispersal determine species distribution. Moreover, while you can discuss about, e.g., the foraging spatial pattern of a single individual, you cannot study an isolated individual's dispersal. There is no meaning of an individual dispersing if there are no other individuals in its world. Dispersal has ecological roots and implications, implicitly or explicitly considered. It is a population- (and above) level process, which at least implicitly takes into account the knowledge of the location of other individuals.

After this terminological discussion, it is convenient to specify in which way the terms regarding movement were used in this text. As previous works have done, this thesis, a theoretical work with a clearly ecological orientation, uses the term 'dispersal' and 'mobility' to refer loosely to the movement and mobility of individuals in the ecological system. Additionally, it is convenient to use the terms 'diffusion' and 'diffusivity', to discuss about the movement of individuals, following the terminology of previous works upon which this one is based. As it can be understood, the aforementioned terms will be used rather interchangeably, and their meaning will be generally context-dependent.

2.2. Complexity in the ecology and evolution of movement

Ecological systems could be considered typical examples of complex systems. They are realized in multiple, inter-linked hierarchical levels. From lower to higher hierarchical levels, we find: the individual, population, metapopulation, community, biome, until the whole biosphere level. As complex systems, a level is characterized by patterns and behaviors which emerge because of the interaction between its below level constituent entities. Additionally, the entities of a level do not exhibit the characteristic patterns and behaviors of the above level they constitute.

The kinds of complexity that can be found in ecological systems are at least six (Loehle, 2004): structural, process, behavioral, geometric, spatial and temporal. Structural refers to the structure of the ecological interactions (like trophic interactions), process refers to multi-step processes (like soil formation), behavioral refers to the complexity of individual behavior (like animal foraging), geometric refers to the geometry of ecological objects (like a three-dimensional forest canopy), spatial refers to spatial patterns of distributions (like vegetation patterns), and temporal refers to temporal dynamics (like population fluctuations).

The last two of the listed kinds of ecological complexity, spatial and temporal, seem to have received greater attention, possibly because of their easily observed results and their practical applications. For example, once homogeneous habitats are transformed into spatially complex landscapes of fragmented habitats, mainly due to anthropogenic disturbance. The visually obvious fragmentation patterns, and the practical urgency for wildlife population conservation, encourages the study of such fragmented ecological systems. To this end, metapopulation models are usually being adopted, in which the interplay between population dynamics and spatial patterns is studied. One of the key processes for the viability of the populations in the metapopulation framework has been found to be dispersal. And it has been shown that the complex interplay between dispersal and the frequency of local extinction emerges not only because of the feedback between spatial and temporal dynamics, but also because of the feedback between spatiotemporal dynamics and dispersal evolution (Ronce and Olivieri, 2004). Hence, a holistic study of dispersal has to take into account the 3-part complex dialogue between spatial dynamics, temporal dynamics, and the evolution of dispersal.

2.3. Dispersal and evolution

The presence of dispersal is ubiquitous in nature. Even the fact that two individuals cannot exist on the same point in space, forces them to disperse passively. But here we care about adaptations, and even then it is fruitless to look for a species whose genes are not able to expand their spatial distribution, either alone or with the help of the environment, in an individual's lifetime or during subsequent generations. Even sessile species, for example think of a typical terrestrial plant species, 'attempt' to colonize available and appropriate habitat by a wide variety of adaptations: the vegetative growth with stolons; the wonderful adaptations of the air, water (and even fire-induced) traveling seeds; or the mutually beneficial 'friendships' with fruit-eating animals. The adaptive advantage of slower or faster dispersal goes beyond colonization (Dieckmann et al., 1999; Ronce, 2007): decrease in extinction risk; less competition between relatives; foraging for food, mating or other resources; avoidance of intraspecific and interspecific competitors (include predators to the latter); decrease in the genetic inbreeding (for the sexually reproducing populations); or exploitation of the spatial and temporal environmental variability. The magnitude of this adaptive armory points to at least two obvious, but worth-recalling remarks: (i) dispersal is heritable (for a study case in butterflies, see Saastamoinen, 2008); (ii) and it is the target of natural, anthropogenic or other kinds of selection Ronce (2007). Thus, dispersal, a principal feature of life, is shaped under various selective forces.

Since dispersal steps with one foot on ecology and with the other on evolution, an interesting approach for the study of its character, nature and dynamics comes under an eco-evolutionary setting. Evidence are accumulating to show that the dialogue between ecology and evolution can take place extremely fast (Carroll et al., 2007), putting to a more suspicious position the old, strict view of discriminating the ecological from the evolutionary time-scales and processes. Thus, focusing on the interplay between ecological and evolutionary dynamics of dispersal seems a promising path. And, this thesis is grounded exactly on that, studying under an eco-evolutionary

setting the evolution of dispersal, and specifically the last of the previous paragraph's list of adaptive advantages of dispersal: the spatial and temporal conditions under which faster or slower dispersal may be selected in an ecological system.

2.4. Spatiotemporal variation and evolution of dispersal

If we search in nature for the extremes of mobility and evolutionary change, we can isolate the two aforementioned forces, spatial and temporal variation, to be at play. On one hand, it seems that slow dispersal may be favored in well-isolated habitats, and hence highly variable in space environments. Take the example of flightless birds, like the New Zealand native kiwis (*Apteryx australis*), on oceanic islands. The loss of the ability to fly has independently evolved several times on oceanic islands, and it seems to have happened in not many generations (McNab, 1994). The reduction in dispersal on such isolated habitats has been observed in plants as well: evolution towards reduced seed dispersal in wind-dispersed short-living weedy plants on the timescale of decades has been shown on inshore islands in British Columbia (Cody and Overton, 1996). On the other hand, the inefficiency of slow dispersing species to withstand, escape or exploit temporally increased or fluctuating competitive, predatory or other environmental pressure is obvious. On the example of the oceanic birds, according to the fossil record, the largest extinction event in the Holocene occurred in the Pacific islands upon human colonization: more than 1,000 bird species, many of them flightless, went extinct due to anthropogenic hunting and habitat loss (Duncan et al., 2013). And, with an example from plants, the species composition was found to be different in soil-disturbed or grazed plots compared to undisturbed ones: more mobile species, reproducing with seeds dispersed by the wind, were occupying disturbed sites; while undisturbed sites were composed mainly by less mobile species, which were reproducing vegetatively (McIntyre et al., 1995). The authors suggested that the ability to colonize open space created after a disturbance event, like heavy grazing, must be favored in such fluctuating environments. In general, it is thought that on one hand spatial variation selects for slower dispersal, and on the other hand faster dispersal is preferable under higher temporal variation, with both of the forces likely acting rapidly in a continuous eco-evolutionary dialogue.

There is a growing body of theoretical literature, concerning the evolution of dispersal rates, which seems to reach to an agreement both in between the theoretical and the empirical studies. On one hand, results have shown that slower dispersers dominate in heterogeneous space (e.g., Hastings, 1983; Dockery et al., 1998; Hutson et al., 2003). With a deterministic, continuous in population size and space model of two competing species in a heterogeneous spatial environment, Hastings (1983) found that the slowest dispersing species wins. Dockery et al. (1998), with the same model, generalized the superiority of slower dispersal in heterogeneous environments beyond two-species competition. On the other hand, studies accumulate to argue for the competitive advantage of faster dispersal under high enough temporal variation (e.g., Hutson et al., 2001; Baskett et al., 2007). The common feature of those studies, in contrast to the deterministic aforementioned model, is the incorporation of population-level stochasticity. For example, Kessler and Sander (2009) illustrated a regime shift towards faster dispersal when the population sizes are sufficiently small. Subsequently, Waddell et al. (2010), with a similar model, reached at the same conclusions for the analytically convenient extremes of dispersal rates, underlining the contribution of demographic stochasticity to the outcome of the competition between species with different dispersal rates. All in all, from both the theoretical and the empirical literature, it seems that spatial and temporal variability are two opposing forces that determine the evolutionary stable dispersal rate under competition: slower dispersers are selected in more spatially heterogeneous environments since colonizing other sites imposes higher risk of ending up on

lower quality space, while faster dispersers are fitter in larger population fluctuations by escaping highly competitive sites and colonizing emptier, less competitive ones.

2.5. Present study

A welcome confirmation of the idea of competition between spatial and temporal variation could come from the study of models with different setting than the usual one. Most of the models used for the evolution of dispersal are patch-based, inspired by the metapopulation framework. They incorporate explicitly an independent variable for the degree of environmental heterogeneity, e.g., as Waddell et al. (2010) did by tweaking the variance of the patch carrying capacity. But spatial heterogeneity without the incorporation of habitat patches is able to arise in a self-organizing manner, by means of aggregated individuals: Hernández-García and López (2004) presented the periodic clustering of individuals with a model in which individuals randomly diffuse, and replicate and die influenced by the local density of neighbors. In a later work, Heinsalu et al. (2013) investigated the outcome of competition between pairs of pattern-forming species differing only in their movement characteristics. They concluded that the species which forms narrower clusters out-competes the other. This finding can be interpreted as additional evidence for the advantage of slower dispersers in heterogeneous environments, and as a promising way to confirm, or reject, in a different modeling setting the contribution of temporal variability.

Inspired by the aforementioned importance of the eco-evolutionary dynamics for the study of ecological systems, and the importance of temporal variation on the evolution of dispersal, this work aimed at two points: (i) To complement the paired, two-species competition setting of Heinsalu et al. (2013), in which they were starting the competitions with equal numbers of individuals. The eco-evolutionary approach the present study followed was a 'simulating real evolution' scheme. This scheme mimics real population evolution, with mutations occurring at reproduction, and letting the system evolve to a possibly existent evolutionary stability. Here, the previous setting of the two competing species was relaxed, and individuals from a continuous range of mobility were allowed to compete. (ii) To investigate the opposition between spatial and temporal variation under the eco-evolutionary setting, and its subsequent contribution to the evolution of mobility.

The two aims of the thesis were achieved by confirming, under the eco-evolutionary setting of simulating evolution: (i) that slower dispersers proved superior, for the parameter values considered by Heinsalu et al. (2013); (ii) that the opposition between temporal and spatial variation was a considerable force of selection in the evolution of dispersal from this model's different perspective. The rest of the thesis is structured as follows. Initially, an overview of the model mechanics and basic behavior will be given (Section "Model"). Next, Section "Basics of spatiotemporal variation" deals with an attempt to identify model input parameters by which spatiotemporal variation can be manipulated. Following, Section "Evolution of dispersal" presents evolutionary experiments. There, by measuring spatiotemporal variation, we will be able to interpret the evolutionary outcomes from the simulations of evolution in terms of the measured spatiotemporal variation, and eco-evolutionary feedback. Finally, the thesis will close with brief conclusions, comments and future perspectives, in Section "Concluding remarks".

3. Model

In this Section, an overview of the model mechanics will be given, as well as a brief description of the main characteristics of its behavior.

3.1. General setting

The model of Heinsalu et al. (2012) conceives a population of individuals existing in a two-dimensional, resource homogeneous, square world of size $L \times L$ with periodic boundary conditions. The point-like individuals are allowed to move, reproduce asexually by fission, and die. Reproductive correlations exist, since upon birth the newborn individual is placed at the parental position. An offspring inherits the movement and demographic characteristics of its parent. The version of the model used here is the one of non-local interaction. According to that, an individual's birth rate may have a linear negative relation, and its death rate a linear positive relation, with the number of other individuals within radius R.

Heinsalu et al. (2013) implemented both a mean-field and an individual-based version of the model, and since here we care about temporal fluctuations, we will focus on the latter, which uses the Gillespie algorithm, described for the specific model in Heinsalu et al. (2012) and in Section "Gillespie algorithm" herein. We will follow the population size, $N(t)$, in continuous time t, starting each simulation with $N(0)$ individuals uniformly distributed in a square domain of $L = 1$, so that the units of length can be interpreted in terms of system size.

3.2. Demography

An individual i reproduces and dies according to Poisson processes with rates r_b^i and r_d^i, respectively. The linear effect of competition on these rates depends on the number of other individuals, N_R^i, the individual i has in distance less than R around it:

$$\begin{aligned} r_b^i &= \max(0, r_{b0} - \alpha N_R^i), \\ r_d^i &= r_{d0} + \beta N_R^i, \end{aligned} \tag{3.1}$$

where r_{b0} and r_{d0} are the intrinsic reproduction and death rates, and $\alpha > 0$, $\beta > 0$ are the parameters introducing the competition. The radius $R < L/2$, so that no neighbor is counted more than once because of the periodic boundaries. The max function ensures that the birth rates do not become negative.

So, the five input parameters for the competition-mediated demography are r_{b0}, r_{d0}, α, β and R.

3.3. Gillespie algorithm

On each simulation step, the following set of actions are accomplished, in effect of increasing or decreasing N by one (Heinsalu et al., 2012): (i) calculate the time to the next step; (ii) choose if the demographic event of the step will be a birth or a death; (iii) select the individual which will realize this event; (iv) execute the event; and (v) move all individuals. The simulation ends either when the time t of a step's occurrence exceeds a specified time t_{end}, or after a specified number of simulation steps.

Since the demographic events follow Poisson processes, the time τ to the next step is sampled from an exponential distribution with parameter

$$R_{tot} = B_{tot} + D_{tot} = \sum_{i=1}^{N} r_b^i + \sum_{i=1}^{N} r_d^i, \tag{3.2}$$

the sum of the birth and death rates of all individuals (Heinsalu et al., 2012). By taking the inverse of the cumulative distribution function of the exponential distribution, we get $\tau = -\ln(u)/R_{tot}$, where u is a pseudo-random number drawn from a uniform real distribution in the interval (0, 1). With probability B_{tot}/R_{tot} the event is reproduction, or else a death will occur. The probability of choosing a particular individual for the specific event is proportional to the individual's contribution to the total of individual rates for that event. For example, if a death is chosen to happen, an individual with higher death rate (i.e., with more neighbors) is more probable to be selected. A death leads to the disappearance of the individual, while a birth means the addition of a new individual on the same spot as the parent, inheriting the parent's characteristics, as was previously mentioned. Finally, all individuals move randomly as it is explained in Section "Movement".

3.4. Movement

For the movement action, the direction of the next jump was randomly chosen from (0, 2π). The individuals were jumping a distance l to that direction drawn from the Lévy-type probability density function:

$$\phi_\mu(l) \approx \tilde{l}^\mu |l|^{-\mu-1}, \tag{3.3}$$

where the space-scale parameter $\tilde{l} \ll l$, and μ is the anomalous exponent controlling the probability of long jumps. The smaller the value of μ, the more anomalous is the diffusion. For $\mu \in (0, 2)$, the variance of (3.3) is divergent, but for $\mu > 2$, the central limit theorem ensures that the distribution of step lengths approaches a Gaussian, at long times. From (3.3), the step lengths were randomly generated by (Heinsalu et al., 2012):

$$l = \tilde{l}\frac{u^{-1/\mu} - 1}{b^{1/\mu}}, \tag{3.4}$$

where u is again a uniformly distributed pseudo-random number in the unit interval, and b adjusts the tail of the distribution in respect to μ. According to Heinsalu et al. (2012), and references therein, $b = [\Gamma(1 - \mu/2)\Gamma(\mu/2)]/\Gamma(\mu)$ in (3.4) was chosen therein such as to agree with previous works. In our case, since our focus was the interval $\mu \in [1, 5]$ which would be continuously visited due to mutations, and for $\mu = 2$ a gamma function in b diverges, we decided to use $b = 1$, without any serious change in the results.

To determine $\tilde{l}$ in (3.4), we start with the case of step lengths drawn from a Gaussian distribution with standard deviation $\tilde{l} = \sqrt{2\kappa/\langle\tau\rangle}$, where a diffusion coefficient κ is defined, and $\langle\tau\rangle = R_{tot}^{-1}$ (Heinsalu et al., 2012). Then, for the Lévy distributed step lengths from (3.3), even though the variance is infinite, a generalized anomalous diffusion coefficient κ_μ can be defined in terms of the space-scale parameter

$$\tilde{l} = (2\kappa_\mu\langle\tau\rangle)^{1/\mu} = (2\kappa_\mu/R_{tot})^{1/\mu}. \tag{3.5}$$

In conclusion, this study used (3.4) for the generation of step lengths (with $b = 1$), where the space-scale parameter was taken from (3.5). So, the movement input parameters were κ_μ and μ.

3.5. Basic behavior

One of the characteristic behaviors of this model, as it was already mentioned, is the self-organized pattern formation. Under suitable parameter values, individuals are met mainly in clusters (Figure 3.1 a and b). Hernández-García et al. (in press) have shown that the distance

c between the clusters is $R < c < 2R$, and the clusters are arranged periodically in a hexagonal pattern (Figure 3.1 a and b). The main reason for this aggregation is attributed to non-local competition, and an extreme example will illustrate the formation of the pattern because of the instability of the homogeneous spatial configuration. Let us imagine an immobile individual in a homogeneous spatial configuration of an immobile population at equilibrium density. Let us consider additionally that the individual lies between two small areas whose distance from it is less than R, the distance between them is more than R, and their density due to fluctuations increases. Then, our individual will receive higher competitive pressure than the individuals in those two areas. The area where our individual lies will get less dense due to harsher competition, and the density on the two areas will increase further because of the decrease in density in between the two areas' space. This positive feedback loop will end with no individuals in between the two areas (the so-called 'death-zone'), and with the two areas becoming local density maxima, i.e., clusters. If we relax the immobility assumption in the example, then the movement of individuals will tend to diffuse away the inhomogeneities created by competition. Thus, the essential mechanism for the explanation of the observed model behavior brings forth the opposition between competition-mediated increase in clustering and mobility-mediated decrease in it (Heinsalu et al., 2012). Heinsalu et al. (2012) showed that by decreasing κ_μ or μ, the linear width of the clusters becomes smaller, the particle density in the clusters higher, the density between the clusters lower, the number of clusters larger, and the average number of individuals increases in consequence (Figures 8, 9, 10 therein; Figure 3.1 herein). Thus, for increasing values of the movement input parameters, μ or κ_μ, we pass from more to less clustered spatial configurations.

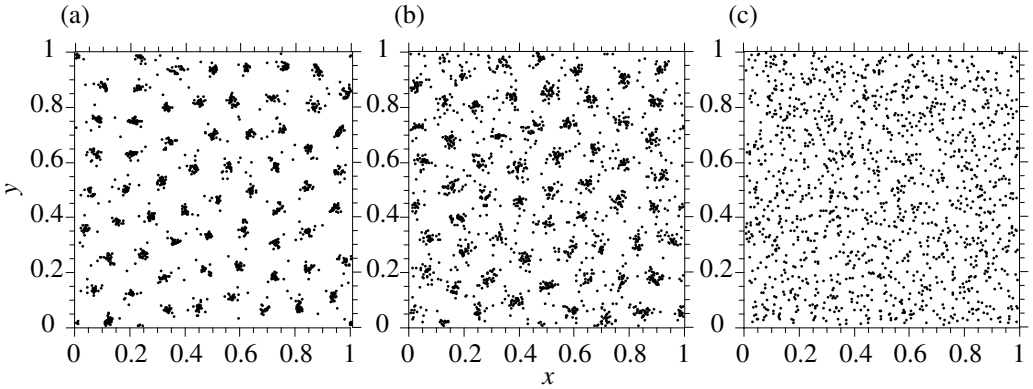

Figure 3.1: Spatial configurations of individuals (black dots) for 3 values of the movement parameter μ. (a) $\mu = 1$; (b) $\mu = 1.3$; (c) $\mu = 3$. Other, common-valued parameters: $\kappa_\mu = 10^{-4}$, $R = 0.1$, $r_{b0} = 1$, $r_{d0} = 0.1$, $\alpha = 0$, $\beta = 0.02$, $N(0) = 1000$. The snapshots were taken at simulation times $t = 5000$, $t = 1000$ and $t = 500$, for (a), (b) and (c), respectively.

As a final but important remark, it is crucial to realize that in this study we care about the evolution of movement strategies in respect to mobility, and not in respect to movement types. We would care about the evolution of movement types if we track the evolutionary change in μ and this could correspond to an evolutionary change in the range of movement types: from the ballistic ($\mu \to 0$), to the Lévy-like ($0 < \mu < 2$), to the Brownian-like movement type ($\mu > 2$). But, by adopting the specific model, with step lengths generated according to (3.4) and (3.5) as it is described in Section "Movement", it seems that lower μ does not mean more anomalous

diffusion with more frequent, longer jumps (Figure 3.2). Since the generated step lengths l, during simulations with the Gillespie algorithm for different μ values, showed a general increase in l with μ (Figure 3.2), we could follow the evolution of mobility by enabling mutations on μ, and by mainly keeping κ_μ fixed. The parameter value set in Figure 3.2 was one of the two typically used settings of the present study (weak competition), and the same qualitative trend arose for the parameter value set of the second setting (strong competition), in similar results not shown here. In conclusion, in the present study, the focal parameter by which an evolutionary change in mobility will be implied is μ, and we will ignore the insignificant differences between movement types arising by the change in that parameter: larger μ, hereon, will mean faster dispersal.

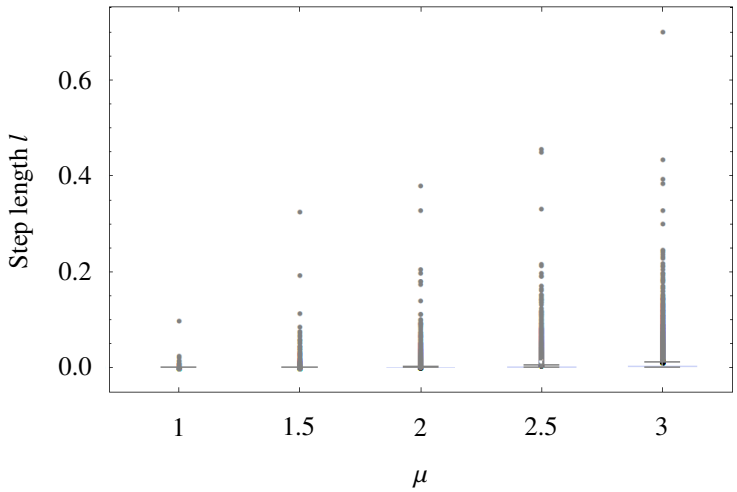

Figure 3.2: Box-and-whisker charts of step lengths l in respect to μ. Black and gray dots represent outliers and far outliers, respectively. Black dashes denote the fences, while light gray longer dashes denote the lower-upper quartiles (barely visible, close to zero). For each μ, $25 \cdot 10^4$ step lengths were taken according to (3.4) and (3.5) as it is described in Section "Movement", during the simulation of an equilibrium population with the Gillespie algorithm. Parameters: $\kappa_\mu = 10^{-4}, R = 0.1, r_{b0} = 1, r_{d0} = 0.1, \alpha = 0.02, \beta = 0, N(0) = 1000$.

3.6. Summary of parameters

Essentially, the model incorporates the following groups of input parameters (apart from the spatial and temporal background): five responsible for the demography (Table 3.1, the first five parameters), two combinations of demographic parameters which will be our main focus (Table 3.1, the following two parameters, between the dashed lines), and two responsible for the movement (Table 3.1, the last two parameters). When we consider the evolution of mobility, one of the two movement parameters essentially changes from an input parameter to a dependent variable.

Table 3.1: Model parameters

Parameter	**Symbol**
Intrinsic birth rate	r_{b0}
Intrinsic death rate	r_{d0}
Effect of density-dependence on birth rates	α
Effect of density-dependence on death rates	β
Neighborhood extend	R
Competition intensity	$\gamma = \alpha + \beta$
Competition's contribution to the death rates	$\delta = \beta/\gamma$
Lévy index	μ
Diffusion coefficient	κ_μ

4. Basics of spatiotemporal variation

This Section aims to: (i) provide the definitions of temporal and spatial variation which will be adopted in the present study; and (ii) retrieve from literature, and investigate possible ways to affect the two types of variation, in terms of model input parameters.

4.1. Temporal variation

We will call temporal variation the variability in the neighborhood density N_R^i in time. To illustrate this, we can take the extreme example of an immobile individual. This individual feels a temporal change in the competitive pressure. After each simulation step, individuals have entered and left its sensing zone of radius R, either because of demography or because of movement. We could say that temporal variation is the variation in N_R^i during time on a fixed location.

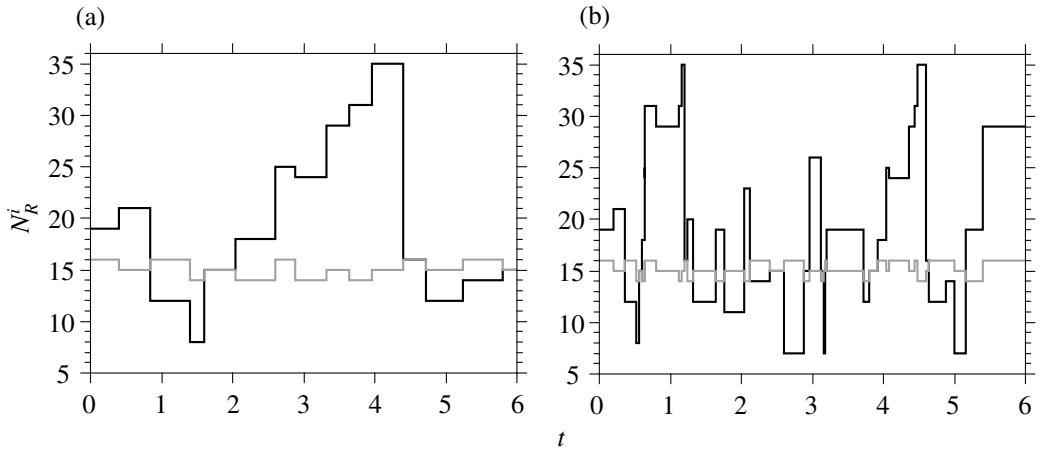

Figure 4.1: Imaginary examples of temporal change in the neighborhood density N_R^i of an individual i. In both Panels, the black and gray lines represent higher and lower, respectively, temporal variation in N_R^i among simulation steps. (a) Smaller mean and variance in the number of steps per time interval. (b) Larger mean and variance in the number of steps per time interval.

Before going further, we must point out that temporal variation seems to have two components. Imagine an immobile individual of an equilibrium population, sensing the competitive pressure in terms of its neighborhood density N_R^i. After a simulation step, during which a demographic event and the movement of all individuals take place, N_R^i might change. One component of variation, then, is the variation in N_R^i among steps (compare the black with the gray line in each Panel of Figure 4.1). The gray line represents lower among steps variation, while the black line represents higher. On the other hand, the number of steps per time interval is not fixed. Thus, the other component of temporal variation would be in terms of the mean and variance of the number of steps per time interval (compare Figure 4.1 a with b). In Figure 4.1 a, smaller mean and variance in the number of steps per time interval is exhibited. Hernández-García et al. (in press), in an attempt to explain the more irregular arrangement of clusters for increased contribution of the competition to the death rates, invoke the second component of temporal variation. They explain that since the birth and death rates follow Poisson processes, the mean and variance in the number of steps per time interval follow Poisson distributions with mean equal to variance

equal to the values of the rates. Thus, increased contribution of the competition to the death rates leads to higher rates, which produce more fluctuating processes in consequence. But, notice that, under the setting of the model, what matters for the survival and prosperity of our imaginary immobile individual is not the number or variation of the number of steps per time interval, but the variation in the competitive pressure it feels. Essentially, at each simulation step a contest among all individuals takes place, and either this contest occurs frequently or not it is the same for the individual, since the time to the next step is the same for all. Thus, in the present study we will concentrate on the first component of temporal variation, the variation in N_R^i among simulation steps.

In the initial attempt that follows, mobility will be neglected, so that the possible influence of the demographic parameters on temporal variation will be revealed. Let us consider, then, a case of population of immobile individuals. The population has reached equilibrium, and pattern formation has occurred. For simplicity, we can assume that the system size L is so small, or that the radius R so large, that only one cluster can be formed. In that cluster, all individuals have the same birth and death rates, $b = r_b^i$ and $d = r_d^i$ respectively, $\forall$ i individual in the cluster. Additionally, since we assumed that we are at equilibrium, $b = d = r_{b0} - \alpha N_R^{eq} = r_{d0} + \beta N_R^{eq}$, where N_R^{eq} is the equilibrium number of neighbors within radius R. From the latter equality of individual rates, it follows that (Hernández-García et al., in press) :

$$N_R^{eq} = \frac{r_{b0} - r_{d0}}{\alpha + \beta}. \tag{4.1}$$

The number of neighbors in equilibrium increases if the sum of the competition's contributions to the rates is decreased, and when the basic birth rate increases in respect to the basic death rate. It is not relevant, for the number of neighbors at equilibrium, if the competition affects the birth or the death rates. What matters is what we will call here 'competition intensity', i.e. the sum $\gamma = \alpha + \beta$. Next, we see that the sums of individual rates are $B_{tot}^{eq} = N_R^{eq} b$, and $D_{tot}^{eq} = N_R^{eq} d$, and consequently $B_{tot}^{eq}/R_{tot}^{eq} = D_{tot}^{eq}/R_{tot}^{eq} = 1/2$, since $b = d$. Thus, the next demographic event is equally probable to be a death or a birth. Also, since all individuals feel the same competitive pressure, all of them are equally probable to be chosen. Now, let us imagine that the next demographic event is a birth. This leads to a decrease of the individual birth rates by α, an increase of the death rates by β, and B_{tot}, D_{tot} and R_{tot} may be affected as well. So, we see that the change in the number of individuals affects the likelihood of the type of the next event. In what follows, an attempt will be made to have a quantitative picture of this relationship in terms of the input parameters. This will be helpful for revealing the way by which temporal variation can be affected by demography in this model.

As the equilibrium number of neighbors N_R^{eq} had increased by one, we saw that this would likely affect the probability of the next event being a death or birth. So, let us generalize now with the probability that the next event will be birth, $B_{tot}^{'}/R_{tot}^{'}$, given a deviation from N_R^{eq} by n, so that n takes negative and positive values, but still not high enough, so that we can leave aside the max() function in (3.1). The new, updated sum of birth rates is

$$B_{tot}^{'} = (N_R^{eq} + n)[r_{b0} - \alpha(N_R^{eq} + n)], \tag{4.2}$$

and

$$R_{tot}^{'} = (N_R^{eq} + n)[r_{b0} + r_{d0} + (\beta - \alpha)(N_R^{eq} + n)]. \tag{4.3}$$

The difference in the probability of the next event being a birth would be

$$\Delta\frac{B}{R} = \frac{B'_{tot}}{R'_{tot}} - \frac{B^{eq}_{tot}}{R^{eq}_{tot}} = \frac{B'_{tot}}{R'_{tot}} - \frac{1}{2}, \tag{4.4}$$

since at equilibrium the two types of events are equiprobable. By using (4.2), (4.3), and finally (4.1), we can arrive at

$$\Delta\frac{B}{R} = -\frac{n(\alpha+\beta)^2}{4(\beta r_{b0} + \alpha r_{d0}) + 2n(\beta^2 - \alpha^2)}. \tag{4.5}$$

Finally, we can express (4.5) in terms of γ and $\delta = \beta/\gamma$, as

$$\Delta\frac{B}{R} = \frac{n\gamma}{4r_{d0}(\delta - 1) + 2n\gamma - 4\delta(r_{b0} + n\gamma)}. \tag{4.6}$$

By putting (4.6) back in (4.4), we retrieve the probability of the next event being birth given the deviation n from the neighborhood equilibrium density N^{eq}_R (Figure 4.2 a). The three curves are for different δ values (0, 0.5, and 1) and $\gamma = 0.02$, with a denser curve representing larger δ. The general trend in all of them is the same: The probability of a birth event increases above one half if we are below equilibrium, and decreases below one half if we are above.

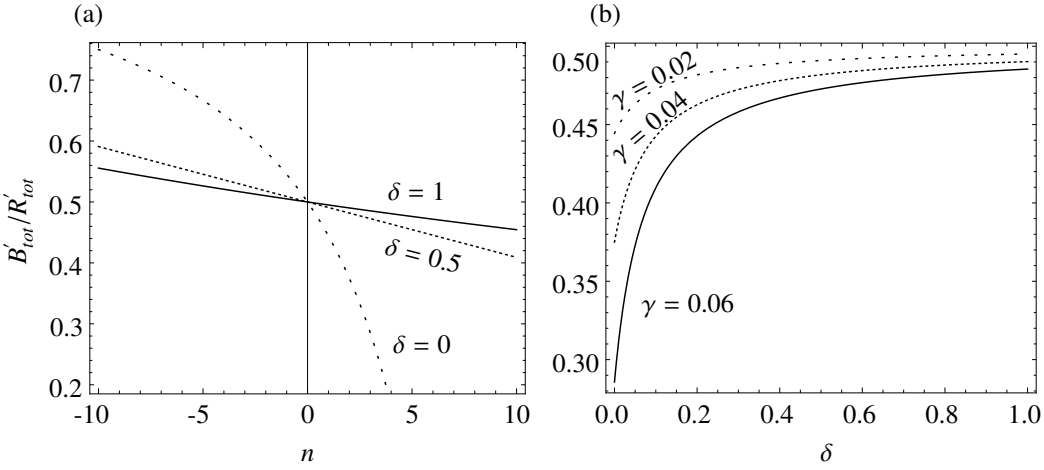

Figure 4.2: Probability of the next demographic event being birth given: (a) the deviation n from the neighborhood equilibrium density N^{eq}_R; (b) the contribution δ of competition to the death rates, for $n = 1$. All individuals were considered immobile, and the whole population was in a single cluster. Other, common-valued parameters: $r_{b0} = 1$, $r_{d0} = 0.1$.

A comparison between the three curves, in Figure 4.2 a, gives the first indication of the way we could affect temporal variation: The smaller is the competition's contribution to the death rates, δ, the steeper is the change in the probability of a birth. For small δ, the addition of individuals results in higher probability of deaths, and the cluster is attracted stronger to the equilibrium density. Thus, we expect smaller fluctuations for smaller δ. In Figure 4.2 b, this trend is shown in a clearer manner. Here the three curves are for different γ values (0.02, 0.04,

and 0.06) and $n = 1$, with a denser curve representing larger γ. As we would have expected based on the previous observations, by increasing δ we must be driven to larger fluctuations. Indeed, in Figure 4.3 a, the positive relationship of temporal variation with δ is shown, after stochastically simulating an ensemble of single-clustered populations. The comparison between the three or the two γ curves in Figures 4.2 b or 4.3 a, respectively, reveals something additional. In more intense competition, i.e. for larger γ, the temporal variation must be lower (Figure 4.3 b). In conclusion, we saw that larger contribution of the competition to the death rates should lead to higher temporal variation, while more intense competition should reduce it.

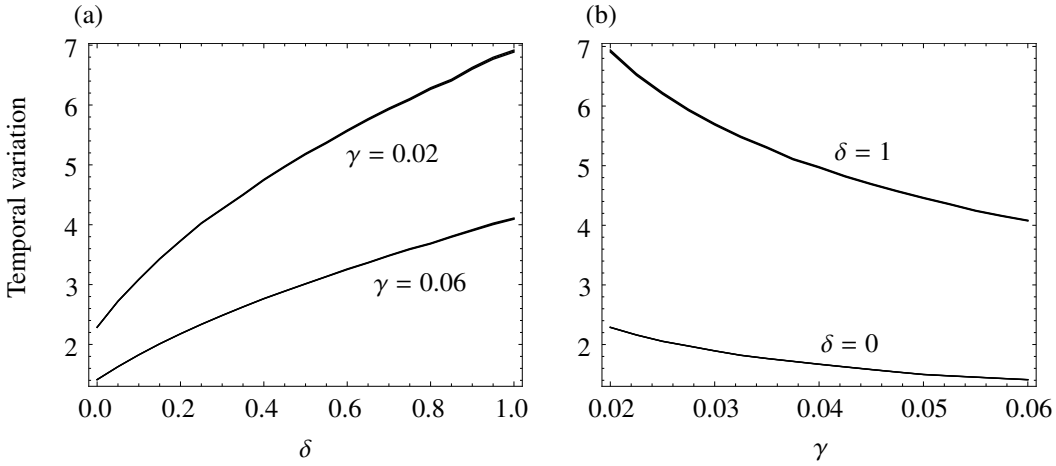

Figure 4.3: Temporal variation, measured as the temporal standard deviation of the number of a single-clustered population's immobile individuals, in respect to: (a) the contribution δ of competition to the death rates; (b) the competition intensity γ. The error of the mean curves overlap with the curves of the mean. Other, common-valued parameters: $r_{b0} = 1$, $r_{d0} = 0.1$.

Movement could be another source of increase or decrease of temporal variation, as individuals abandon and enter sensing zones by moving around. We could expect that higher mobility tends to homogenize the temporal variations created by demography. Recall that the way we explained the adaptive advantage that faster dispersers enjoy in fluctuating environments was exactly the exploitation of emptier locations and the avoidance of crowded ones. If they have been selected for that, then fast dispersers should tend to smooth the large deviations created by a more fluctuating demography. We will have the opportunity to see in the numerical simulations that this relationship should not be expected to be monotonous when mobility is incorporated, at least for the parameter values considered. But, indeed, sufficiently high μ could enforce its own temporal variation on immobile sensing zones of radius R.

All in all, we saw that temporal variation must be affected by both demography and movement. About demography, the positive and negative effect of increasing δ and γ, respectively, was shown. For movement, we were limited to speculations, even though later results will reveal the rather intricate nature of its inclusion in the dynamics, at least for the parameter values tested.

4.2. Spatial variation

By spatial variation we recognize here the variability that is exhibited in the number of neighbors N_R^i as an individual i moves around. We can take the extreme example of a single, super-

mobile individual. This individual is so fast that it can scan all the spatial domain so that time can be considered frozen, and like the rest of the population stands still. Thus, this individual will experience fluctuations in the competitive pressure as it travels. And this is what we refer here when talking about spatial variation: the variability in N_R^i across space in a slice of time.

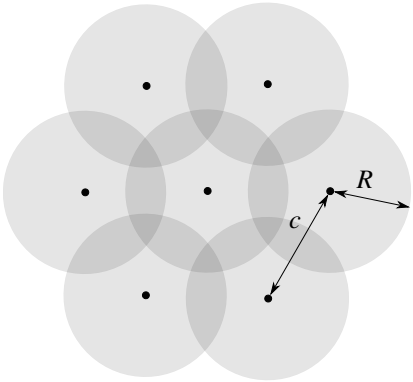

Figure 4.4: Example spatial configuration of clusters of individuals (the black dots) arranged hexagonally. Each cluster possesses a gray disk of radius R centered on it. If an individual lies on a disk, it receives the competitive pressure from the individuals of that disk's cluster. In the specific example, the inter-cluster distance $c = 1.5R$.

The example of the immobile population proved useful for the indication of the effect of δ and γ on temporal variation. Here, for the investigation of spatial variation, we will imagine again an immobile, clustered, equilibrium population. No individuals can be met between the clusters, and the clusters are so narrow that they can be considered points. That is, all individuals of a cluster are at the same location. Since the clusters are arranged periodically (Hernández-García and López, 2004), we could focus on only one set of seven clusters (Figure 4.4). A gray disk can be thought as the area under which if an individual lies, it feels the competition of that cluster's individuals. Because of the periodicity of the pattern, we can focus only on the central cluster and its disk, and imagine a super-diffusive individual moving randomly on that disk. It is apparent that there are various parts on that disk that if the individual steps on, it will receive the competitive pressure from 1, 2, or maximum 3 clusters. Given the radius R and the inter-cluster distance c, we can calculate the fractions of the disk's area which are overlapped by another two, one, or no disks. Our super-mobile individual has a probability to land on a spot from which it will receive competition from 3, 2, or 1 clusters weighted by the fractions of the respective areas. For the specific example of Figure 4.4, the calculated fractions for the 3-, 2- and 1-cluster reach areas were approximately 0.159, 0.547 and 0.294 of the disk area, respectively. The equilibrium number of individuals on a cluster, since we are at equilibrium and we had neglected mobility, comes from (4.1). And since we have already seen that δ and γ influence temporal variation, we can check their effects on the spatial variation that our individual senses by stochastically running our limited system for various values of δ and γ. From a generated list of N_R^i, we take the standard deviation as a measure of spatial variation of N_R^i. In consequence, spatial variation was found to increase with δ (Figure 4.5 a), and decrease with γ (Figure 4.5 b).

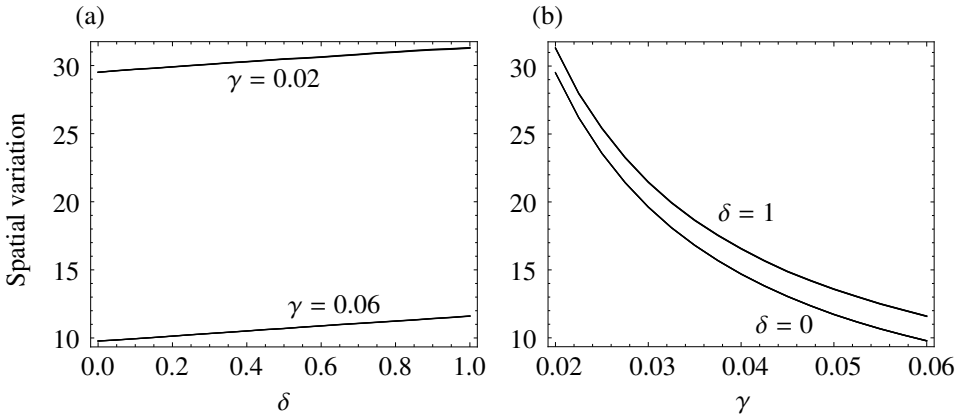

Figure 4.5: Spatial variation, measured as the standard deviation of the number of neighbors exhibited to an individual which was randomly moving into the disk of the central cluster in Figure 4.4, in respect to: (a) the contribution δ of competition to the death rates; (b) the competition intensity γ. The error of the mean curves overlap with the curves of the mean. Other, common-valued parameters: $r_{b0} = 1$, $r_{d0} = 0.1$.

Let us go on now to the effect of mobility. It was already mentioned that for increasing values of the movement input parameters, μ or κ_μ, we pass from more to less clustered spatial configurations (Figure 3.1), and we could link higher values of these parameters with faster dispersal. Apart from the visual comparison of the degree of spatial homogeneity, the degree of clustering can be calculated with various ways. One example attempted here was by means of k-nearest neighbors. Upon reaching equilibrium, and after each moving action, the total distance to the 4-nearest neighbors of each individual was measured. Comparably, the same was done for an ensemble of uniform spatial distributions with the same $N(t)$. The total distances were averaged among individuals, and the ratio of the mean among the random ensemble's individual average to the real individual average was kept. Finally, a temporal average was taken, and the same procedure was done for an ensemble of simulations. From this attempt, the mean ratio values for the range $\mu \in [1, 3]$ of Figure 3.1, were decreasing for increasing μ (Figure 4.6 c). Thus, larger values of the movement parameters decrease clustering, and, possibly, spatial variation in consequence.

Apart from the negative relationship of clustering with μ, a comparison of the three Panels in Figure 4.6 reveals an additional trend, which was studied in Heinsalu et al. (2012): for increased contribution of the competition to the death rates, clustering increases. Specifically, if we fix the sum γ, increased δ leads to increased clustering especially for lower values of μ (Figure 4.7). For higher δ, smaller number of individuals is found on the death zones. This happens because, as Heinsalu et al. (2012) have shown, the distance c between the clusters is $R < c < 2R$, and these individuals may feel the pressure from more than one cluster. When competition affects more the death rates, then the individuals in the death zones are more probable to be eliminated. If the competition was mainly in the birth rates, these individuals may not have reproduced, but they would not have being dying so frequently in respect to others either. That is a reason why higher clustering is observed for larger δ. We saw earlier, in Figure 4.5 a, that δ may affect spatial variation, and here we learned that it may affect spatial variation indirectly by influencing spatial clustering.

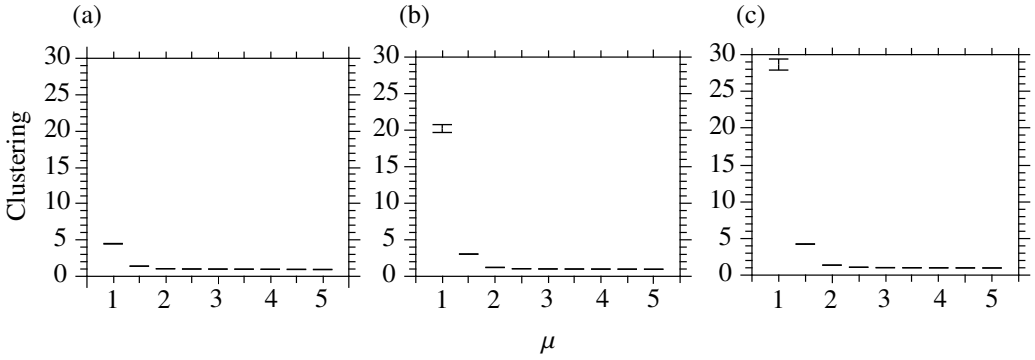

Figure 4.6: Clustering in respect to μ for three values of the competition's contribution to the death rates, δ, under strong competition γ. A uniform spatial configuration has a clustering value equal to 1. Details of the clustering's calculation method can be found in Section "Spatial variation". (a) $\alpha = 0.06$, $\beta = 0$; (b) $\alpha = 0.03$, $\beta = 0.03$; (c) $\alpha = 0$, $\beta = 0.06$. The error bars denote the error of the ensemble mean. Other, common-valued parameters: $\kappa_\mu = 10^{-4}$, $R = 0.1$, $r_{b0} = 1$, $r_{d0} = 0.1$, $N(0) = 1000$.

In conclusion, spatial variation was found to be positively and negatively influenced by δ and γ, and that clustering is affected by both demography and mobility. Larger δ and smaller μ lead to higher clustering. But we have to keep in mind that higher clustering may not be synonymous to higher spatial variation. The way of measuring clustering, at least in this study with the k-nearest neighbors, is in terms of the distances between closer individuals. But, according to our definition of spatial variation, an individual's world is within radius R. As we will see later, the agreement of clustering with the measured spatial variation in the numerical simulations is not much faithful.

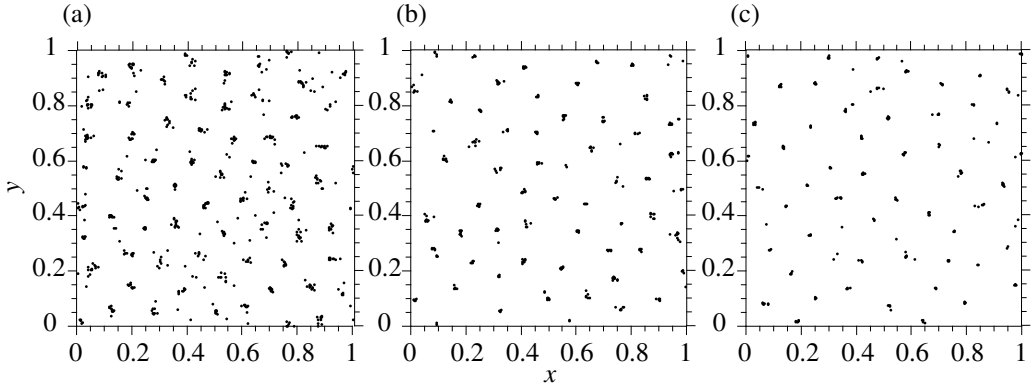

Figure 4.7: Spatial configurations of individuals (black dots) under 3 values of δ, the competition's contribution to the death rates. (a) $\delta = 0$; (b) $\delta = 0.5$; (c) $\delta = 1$. Other, common-valued parameters: $\kappa_\mu = 10^{-4}$, $\mu = 1$, $R = 0.1$, $r_{b0} = 1$, $r_{d0} = 0.1$, $\gamma = 0.06$, $N(0) = 1000$. The snapshots were taken at simulation times $t = 1000$, $t = 300$ and $t = 100$ for (a), (b) and (c), respectively.

4.3. Temporal over spatial variation

Until now, we have concluded that increased weight of the competition to the death rates, δ, increases both kinds of variations. On contrary, more intense competition, γ, was shown to reduce both kinds of variation. But, in this study, which is about the evolution of dispersal, what we should care mainly is the relative difference between the two kinds, according to the literature. We could take a look at how the ratio of temporal over spatial variation is affected by the two demographic parameters considered in this Section. The effect of mobility on the ratio will be investigated only on the numerical simulations of evolution. Contrary to what has been found for the two kinds of variation independently, by either increasing δ or γ the relative size of temporal variation increases in respect to spatial variation (Figure 4.8 a and b). Thus, we should expect that for increasing δ or γ evolution will tend to higher mobility.

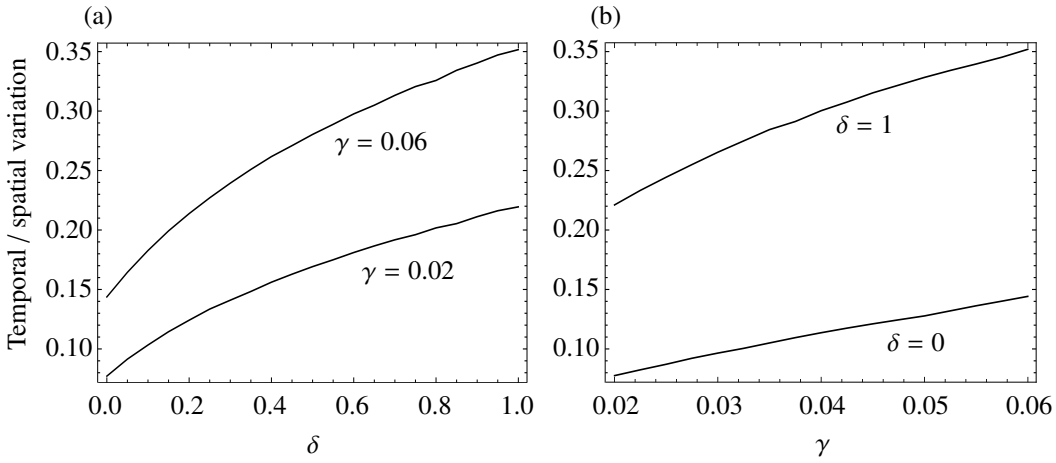

Figure 4.8: Temporal over spatial variation, calculated from the mean of temporal and spatial variation of Figures 4.3 and 4.5, respectively, in respect to: (a) the contribution δ of competition to the death rates; (b) the competition intensity γ.

5. Evolution of dispersal

Section "Basics of spatiotemporal variation" managed to extract three input parameters by which spatial and temporal variability should be influenced: (i) the intensity of competition, defined as $\gamma = \alpha + \beta$, with α and β from (3.1); (ii) the competition's contribution to the death rates, defined as $\delta = \beta/\gamma$; and (iii) both of the movement parameters, μ and κ_μ. The influenced spatiotemporal variation, according to literature, is expected to affect the outcomes of dispersal evolution. Thus, by manipulating the aforementioned parameters, we aim to test if the subsequent change in spatiotemporal variation will lead to a different evolutionary outcome. The numerical, evolutionary experiments manipulated two competition intensity levels (strong and weak competition, $\gamma = 0.06$ and $\gamma = 0.02$, respectively) and a limited number of the competition's contribution to the death rates (principally, the two extremes $\delta = 0,\ 1$). The effect of the other parameters has not been investigated, and thus held fixed: $R = 0.1$, $r_{b0} = 1$, and $r_{d0} = 0.1$. Additionally, $\kappa_\mu = 10^{-4}$ will be generally held as such, except from one case where we will take a look at the evolution of κ_μ in populations with fixed $\mu = 3$. Thus, we will focus on the effect of δ and γ from the demographic input parameters, and mainly the effect and evolution of μ from the movement parameters. Notice that, because of the continuously applied eco-evolutionary dynamics, the relation of μ with spatiotemporal variation should be bidirectional: μ should influence spatiotemporal variation (the ecological counterpart of the dynamics), and at the same time spatiotemporal variation is expected to affect μ (the evolutionary counterpart). The experimental setting aimed to elucidate: (i) the effect of the contribution of competition to the death rates under strong competition; (ii) the effect of the contribution of competition to the death rates under weak competition; and (iii) the effect of competition intensity for a given contribution of the competition to the death rates. The effects of these treatments will be considered under two main approaches: (i) by inspecting the temporal change in the distribution of individual mobility of evolving populations; and (ii) by measuring the temporal and spatial variation of evolving and non-evolving populations.

The rest of this Section is structured as follows. First, details will be given regarding the methodology of the evolutionary simulations. And next, we will approach the evolution of mobility from the three aforementioned treatments: under "Strong competition", under "Weak competition", and by a "Weak-strong competition comparison".

5.1. Methodology

5.1.1. Measuring variation

Spatial variation was defined as the variation in the number of neighbors within radius R, N_R, across space in an instance of time (Section "Spatial variation"). Temporal variation was then defined as the variation of N_R in a fixed location as time goes by (Section "Temporal variation"). For the present study, the standard deviation of N_R was used as a measure for both types of variation. For both types of variation, the same setting was implemented: 25 sensing disks of radius $R = 0.1$, fixed in space, regularly arranged in the $L \times L$ domain of $L = 1$. The arrangement was such that there was no overlap between the areas each sensing zone was covering (Figure 5.1). The center of the bottom left zone was at (0.1, 0.1), and the subsequent centers were placed at intervals of 0.2, both in the horizontal rows and vertical columns. Of course, this is one way of arranging the static sensing zones, and someone could argue that maybe a random distribution of zones, and a larger number of them, would be more appropriate. Even if it is, something that was not tested in this study, the important thing is that we compare measurements under the same setting, and a difference in variation, if any, should be detected across treatments. For

the spatial variation, the standard deviation of N_R, s_{sp}, between the 25 disks was calculated after each simulation step. In a simulation without evolution, the equilibrium temporal average of s_{sp}, $\bar{s}_{sp}$, was kept. The final measure was $\langle \bar{s}_{sp} \rangle$, an ensemble average from independent simulations. If evolution was taking place, then s_{sp} was temporally averaged at subsequent intervals of a specified number of steps. For the temporal variation, the temporal standard deviation of N_R, s_t, for each one of the disks was calculated. For a specified number of steps upon reaching equilibrium, the average between the 25 disks, $\bar{s}_t$, was kept. The final measure was $\langle \bar{s}_{st} \rangle$, an ensemble average. If evolution was taking place, then s_t was spatially averaged between the 25 disks for subsequent intervals of a specified number of steps. Finally, to compare the sizes of spatial and temporal variation, the ratio of the temporal over the spatial variation was taken: for each simulation, $\bar{s}_t / \bar{s}_{sp}$ was kept, and then it was averaged from an ensemble.

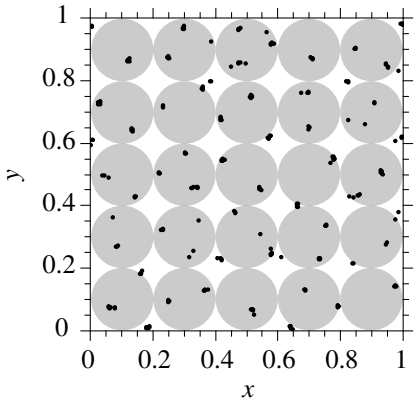

Figure 5.1: Spatial configuration of the 25 sensing zones of radius $R = 0.1$, for the measurement of temporal and spatial variation. The sensing zones are depicted as gray disks, on an example spatial configuration of individuals (clusters of black dots).

5.1.2. Simulating evolution

Simulating evolution focuses on the evolution of phenotypic traits, and its main advantage lies exactly on that: it tackles the now acknowledged complexity of the genetic contributions, by studying the dynamics of their end-result alone: the phenotype. A phenotypic trait, a general and all-in-all term, is any characteristic of an organism that can be studied. For example, you can consider as phenotypic traits the color of your eyes, the length of giraffes' necks, the aggressiveness of baboons, and for us here the mobility of the digital individuals. The mechanisms that give rise to these traits can be complex, and many times still unknown. Instead, with this scheme, all these intricacies are omitted, and we focus on the selection of phenotypic traits, not genes. Another advantage is that it links population dynamics with evolutionary change, in agreement with contemporary findings (Carroll et al., 2007).

This approach attempts to simulate real evolution. The principal idea is to introduce mutations in an already established population. The successful mutants can invade in an ecological setting shaped by the resident, and, by their turn, alter the environment. Thus, an interplay occurs between population and evolutionary dynamics. We consider the evolution of one trait, either μ or κ_μ, while keeping the other fixed. We start with an equilibrium population of all individuals having the same value for the evolving trait. The offspring inherit the parents' characteristics

except for the evolving trait which is allowed to mutate its value. The mutation is an increase or decrease of the parental trait value, drawn from a uniform interval. Because the range of the evolving trait is pre-specified, if a mutation results in a value greater or less than the maximum and minimum of the range, the trait takes the value of that extreme. The simulations are left enough time to reach the evolutionary stable distribution of the trait, if any.

The simulations of evolution are depicted here mainly in plots of temporal change of a trait's distribution. Thus, for each plot, one evolutionary trajectory is shown. The conclusions of this study seem to be based on those single trajectories. The fact is that for each evolutionary trajectory shown here, 9 more were run for replication. A qualitatively similar evolutionary outcome was observed in all other repetitions, for each simulation shown in this study. Hence, the single evolutionary trajectory shown here for each case should be considered a decent representative.

5.1.3. Programming implementations

The programs of this study were encoded in C++. For the generation of pseudo-random numbers, the Mersenne twister random number engine was used, from the `<random>` library introduced in the C++ 2011 standard. Most of the computation time was consumed at the calculation of the number of neighbors, N_R^i, since after each moving action, N_R^i had to be recalculated for all individuals. For this, the KDTREE2 module (its C++ counterpart), a free and open-source software, was assigned with the counting of neighbors (Kennel, 2014). Considerable amount of time was also saved by running independent simulations in parallel with the help of GNU Parallel (Tange, 2011), a shell tool for executing jobs in parallel. It could manage the continuous assignment of jobs to the cores, controlling the combinations of all input values, writing the program output to files, and all these in a single shell line.

5.2. Strong competition

In this Section, we will consider stronger competition ($\gamma = 0.06$) in respect to the next Section's weaker competition setting (there $\gamma = 0.02$). The influence of dispersal evolution by the competition's contribution to the death rates will be investigated. Initially, it will be investigated by observing the temporal change of individual mobility during simulations of evolution. And next, the simulations of evolution will be interpreted in terms of measured spatiotemporal variation of non-evolving and evolving populations.

Let us start with the case of the competition not affecting the death rates at all, $\delta = 0$. We will take a look at the evolution of μ, starting from either $\mu = 1$ or $\mu = 2$ of our predetermined range $\mu \in [1, 3]$. Starting from $\mu = 1$, and allowing mutations after the population had reached equilibrium, no net evolutionary change had been observed, apart from the right tail of the μ distribution because of the continuous production of mutations (Figure 5.2 a). With this initial condition, the evolutionary stable mobility was the lowest allowed. If starting from $\mu = 2$, and again allowing mutations upon reaching equilibrium, the distribution was driven to the highest μ allowed (Figure 5.2 b). The evolving population ascended in μ values, and then it was wandering rather undirectionally in the $\mu \in [2, 3]$ range. Thus, in stronger competition ($\gamma = 0.06$) affecting only the birth rates ($\delta = 0$), slower dispersal was selected in a lower mobility range, and faster dispersal was selected in a higher mobility range, for the parameter values considered.

Let us continue now with the $\delta = 1$ case, competition affecting only the death rates. If the initial $\mu = 1$, the population was evolving to the highest mobility (Figure 5.2 c), in contrast to the respective case of competition not affecting the death rates, $\delta = 0$, where it stayed at the lowest mobility (Figure 5.2 a). Thus, by redirecting the total contribution of competition from

the birth to the death rates, evolution was redirecting the evolutionary stable μ from its lowest to its highest value. Notice, additionally, the greater speed and apparent directionality exhibited by the evolving μ distribution as soon as its main volume had passed $\mu \approx 2$, in comparison with the slower mobility regime of $\mu < 2$ (Figure 5.2 c). Of course, if all individuals were starting with $\mu = 2$, again the population was driven to $\mu = 3$, if competition was affecting only the death rates (Figure 5.2 d). But, this time the greater speed and directionality of approaching and staying at the maximum μ, in comparison to the lower speed and undirectionality exhibited in the case of competition affecting only the birth rates (Figure 5.2 b), was apparent.

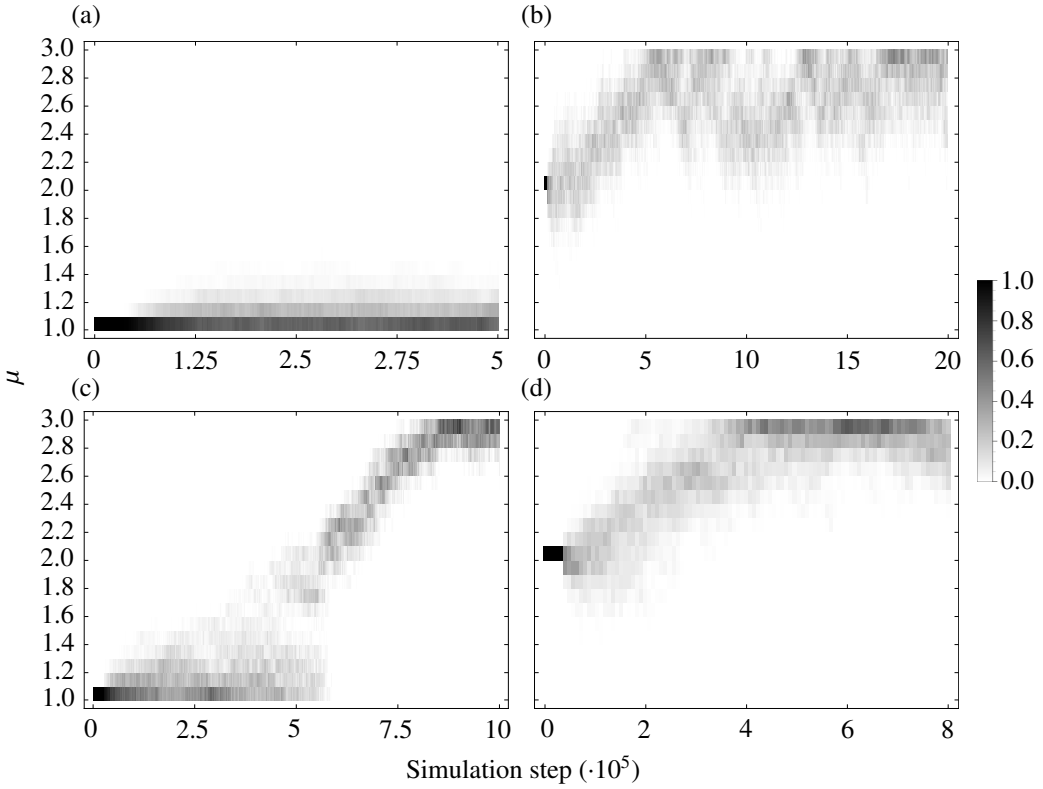

Figure 5.2: Temporal change in the distribution of μ during simulations of μ evolution, under strong competition ($\gamma = 0.06$). The distributions are depicted vertically, where darker color, according to the legend, denotes higher relative frequency of μ in the bins. (a) and (b) competition affecting only the birth rates, $\delta = 0$, and starting with all individuals having $\mu = 1$ and $\mu = 2$, respectively; (c) and (d) competition affecting only the death rates, $\delta = 1$, and starting with all individuals having $\mu = 1$ and $\mu = 2$, respectively. In all simulations, mutations were allowed upon reaching equilibrium. The individuals' offspring were mutating their μ by a quantity drawn uniformly from the interval $(-0.05, 0.05)$. Other, common-valued parameters: $\kappa_\mu = 10^{-4}, R = 0.1$, $r_{b0} = 1$, $r_{d0} = 0.1$, $\gamma = 0.06$, $N(0) = 1500$.

We saw that when competition was impacting only the birth rates, the evolutionary stable mobility was the lowest if starting from $\mu = 1$, but this changed if the initial $\mu = 2$ (Figure 5.2 a and b). Moreover, when competition was affecting only the death rates, $\delta = 1$, then the

evolutionary trajectory was moving to higher mobility even starting from $\mu = 1$, and for initial $\mu = 2$ the path towards higher mobility was even more rapid and determined (Figure 5.2 c and d). We have compared the outcomes for the two extremes of δ, but we could be less rough by taking more, intermediate values of δ, and by starting each simulation of evolution from $\mu = 1$. Thus, we could identify a shift in the selection towards higher mobility. Even though it is a rough attempt to identify the change in the selection of dispersal, for $\delta \in (0.5, 0.67)$, or else for $\beta \in (0.03, 0.04)$ and higher, $\mu = 1$ was not evolutionary stable anymore, and higher μ had the advantage (Figure 5.3 a). As a final remark, someone could object that the evolutionary outcomes which this study considers until now are on the evolution of μ. Thus, the results may have to do with the movement type, as we pass from the Lévy-like movement of $\mu = 1$ to the Brownian-like of $\mu = 3$. As a limited attempt to cast away such doubts, the evolutionary equilibrium distributions of κ_μ, for $\mu = 3$, starting from the lowest κ_3, are shown in Figure 5.3 b. The same qualitative pattern arose: at some interval of δ, a shift was observed from the lowest to the highest diffusion coefficient κ_3.

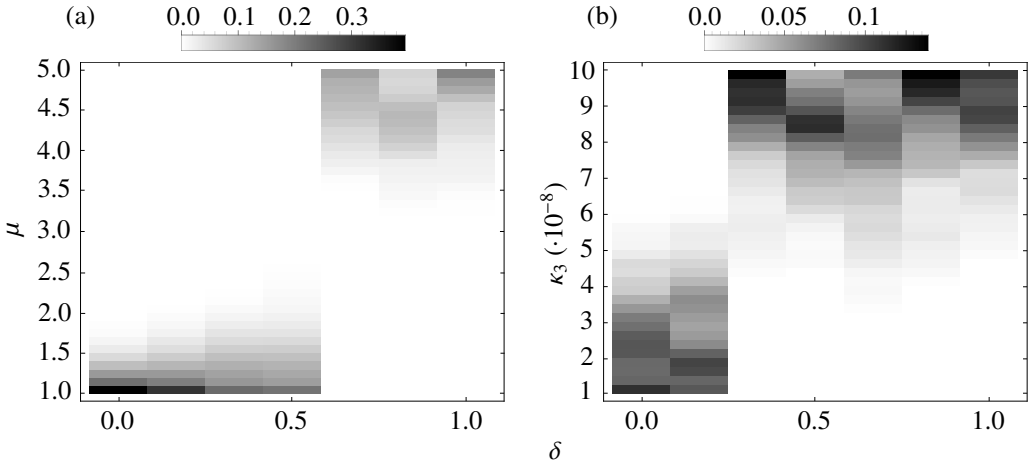

Figure 5.3: Evolutionary equilibrium distributions of the movement parameters μ (a) and κ_3 (b) for various degrees of the competition's contribution to the death rates, δ, under strong competition, γ, and starting from lowest mobility allowed. The distributions are depicted vertically, where darker color, according to the legends, denotes higher mean relative frequency of μ or κ_3 in the bins. For each δ, a single simulation of evolution was carried out, starting with $\mu = 1$ or $\kappa_3 = 10^{-8}$, and mutations were allowed upon reaching equilibrium. Each rectangle is the temporal mean for a duration of $t = 1000$, sampled every $t = 5$, after the distribution had reached a final, relatively unchanged state. The individuals' offspring were mutating their μ or κ_3 by a quantity drawn uniformly from the intervals $(-0.05, 0.05)$ and $(-10^{-9}, 10^{-9})$, respectively. (a) $\kappa_\mu = 10^{-4}$; (b) $\mu = 3$. Other, common-valued parameters: $R = 0.1$, $r_{b0} = 1$, $r_{d0} = 0.1$, $\gamma = 0.06$, $N(0) = 1500$.

By considering all the previous observations of this Section, two trends seem to emerge. First, for a given contribution of competition to the death rates, δ, evolution in a lower mobility regime was attracted stronger to the lowest mobility. By this remark we could justify: the shift in mobility selection, from lower to higher mobility, if starting from lower or higher mobility with $\delta = 0$ (Figure 5.2 a and b); and the more determined and rapid character of evolutionary convergence as the μ distribution had passed $\mu \approx 2$ with $\delta = 1$ (Figure 5.2 c). Second, for a given

mobility regime, increasing the competition's contribution to the death rates, lead to stronger attraction to higher mobility. By this remark we could justify: the departure of the evolutionary trajectory from the low mobility end, $\mu = 1$, when δ was larger (Figure 5.2 a and c); and the thinner and more stable left tail of the distribution at the maximum mobility end, when δ was again larger (Figure 5.2 b and d). As an additional remark, in none of the simulations was an intermediate mobility found to be evolutionary stable. Evolution was leading either to an end of the considered mobility range, or it was wandering in a higher mobility range. Later, based on the measured spatiotemporal variation and the eco-evolutionary dynamics at play, we will discuss why an intermediate mobility would be impossible to be evolutionary stable in the present study and model. All the aforementioned interpretative attempts, still on a rather pattern-based level, are preparing us to turn to a deeper explanation of the patterns and trends observed, based on the opposition of spatial and temporal variation, and the idea of eco-evolutionary feedback.

It was said previously that $\mu \approx 2$ seemed to act as a border separating two different evolutionary behaviors, when competition was not influencing the death rates, $\delta = 0$. On its left, significantly stronger selective forces where acting to hold the population to the lowest mobility (Figure 5.2 a and b). According to the mean-field approach of the model in Hernández-García et al. (in press), for these parameter values, pattern-forming instability occurs at $\mu \approx 1.81$. This could suggest that an abrupt change in spatial variation due to a change in clustering would be the reason for this sudden change in the strength of the selective force. Indeed, measured by the 4-nearest neighbors method presented in Section "Spatial variation", clustering seemed to dissolve rapidly to the uniform spatial distribution across the interval $\mu \in [1, 2]$ (Figure 4.6 a). A mechanistic explanation based on clustering, for the evolutionary behavior in the $\mu < 2$ range, could be that below $\mu \approx 1.8$ a clustered population was resistant to more mobile mutants, since the latter ended up more often in the death zones (Heinsalu et al., 2013). On contrary, in the $\mu > 2$ range, the spatial configurations were rather uniform, and therefore the evolution had redirected towards higher mobility.

For the $\delta = 1$ case (competition only on the death rates), we saw that in both mobility regimes, faster dispersal was selected positively (Figure 5.2 c and d). We could invoke again the pattern-forming instability and its subsequent clustering to explain this case. But here we meet a controversy: Clustering for this setting, and according to the 4-nearest neighbors method, has again its maximum value at $\mu = 1$, and decreases fast towards uniformity to $\mu = 2$ (Figure 4.6 c). Moreover, compared with the case of competition solely to the birth rates $\delta = 0$ (Figure 4.6 a), clustering for $\delta = 1$ is larger in the lower μ values. In this case, the explanatory use of clustering is problematic, since even in the highly clustered regime of $\mu = 1$ and $\delta = 1$, faster dispersers had the advantage. Hence, here we expect that another selective force is at play. The incorporation of temporal and spatial variation, as we defined them in Sections "Temporal variation" and "Spatial variation", will prove a satisfactory way to interpret evolutionary outcomes. First, we will expose the conclusions and speculations appeared in Sections "Temporal variation", "Spatial variation" and "Temporal over spatial variation" to the measured temporal and spatial variation of non-evolving equilibrium populations.

About temporal variation, the positive relationship of temporal variation with the competition's contribution to the death rates, δ, was shown back at Section "Temporal variation", by neglecting mobility (Figure 4.3 a, for $\gamma = 0.06$). In simulations of non-evolving populations at equilibrium, where mobility was also incorporated, generally the same positive relationship was observed (Figure 5.5 b): for a given low value of μ, temporal variation was increasing with δ. A similar trend was not observed for higher values of μ, but this is expected since lower values of μ resemble more the neglected mobility assumption of Section "Temporal variation". Next, the

negative relationship of temporal variation with competition intensity γ (Figure 4.3 b), will be postponed at Section "Weak-strong competition comparison" for the later comparison between the two competition intensity regimes. Lastly, we guessed back in Section "Temporal variation" that increasing mobility may tend to alleviate high temporal fluctuations. Indeed, this was observed for larger δ, in Figure 5.5 b (for $\delta = 1$). Generally, for a given δ, temporal variation, starting from $\mu = 1$, was reaching a local maximum at $\mu \approx 1.5$, then decreasing until $\mu \approx 2$, and finally it was reaching an asymptote value of around 3.9. The minimum of temporal variation located at $\mu \approx 2$, and generally the whole trend, is intriguing. But, as long as the achievement of this study's goals is not interfered by this interesting phenomenon, we will leave it aside. In conclusion, even without neglecting mobility, higher contribution to the death rates, δ, was coupled by higher temporal variation. And movement by its own was following a non-monotonous pattern, even though at high mobility it was imposing specific temporal variation, independently of the competition's contribution to the death rates.

About spatial variation, in Section "Spatial variation" the positive relationship of the competition's contribution to the death rates, δ, was shown for a simplified system (Figure 4.5 a, for strong competition $\gamma = 0.06$). In the present Section, the measured spatial variation of non-evolving populations, for $\mu = 1$ which resembles more the neglected mobility assumption, was reaching an asymptote with δ (Figure 5.5 c). Heinsalu et al. (2012) showed that the distance c between the clusters is $R < c < 2R$, and that clustering increases with increasing δ, as we saw here (Figure 4.6). By these two considerations we can understand that for larger δ, spatial variation increases as the inter-cluster space is emptying. But at the point when almost all individuals are met only in the clusters, spatial variation cannot increase more, since a disk of radius R thrown on a periodic clustered arrangement, with the aforementioned limited inter-cluster distances, has a specific range of number of clusters that can capture beneath it. For larger μ (Figure 5.5 c), spatial variation had a continuous increase with δ, but this continuous increase was getting weaker for increasing μ. Thus, as with temporal variation (Figure 5.5 b), for a given δ and increasing μ, spatial variation was reaching an asymptote value of around 3.9–4, indicating that independently of δ, higher mobility imposes not only a specific temporal but also a specific spatial variation (and notice that the asymptote values of both kinds of variation are similar). About the effect of γ on spatial variation, it will be discussed on the relevant Section "Weak-strong competition comparison". Another notice, we speculated that clustering and spatial variation may not be synonymous. If we compare Figure 4.6 a, and Figure 5.5 c (for $\delta = 0$), we will reveal the difference. While clustering decreased monotonously, spatial variation decreased until $\mu = 2$, and then increased again towards the plateau of a value around 3.9–4. Thus, again the intriguing pattern of the local minimum at $\mu = 2$ appeared when we included mobility, and it could denote the significance of the critical value of $\mu \approx 1.81$ for pattern formation. For the larger $\delta = 1$ in Figure 5.5 c, the monotonous decrease of spatial variation resembles qualitatively the one of clustering, but based on smaller δ, we could say that clustering does not exhibit the same behavior as spatial variation. All in all, we saw that spatial variation reaches an asymptote with increasing mobility, its relationship with δ depends on μ but generally was found positive here also, and that clustering cannot capture spatial heterogeneity in the way individuals perceive it. Consequently, it is suggested that clustering would not be a helpful measure for the study of the evolution of mobility with this model.

Finally, regarding the ratio of temporal over spatial variation, in Section "Temporal over spatial variation" it was shown that it follows a positive relationship with the competition's contribution to the death rates (Figure 4.8 a, for $\gamma = 0.06$). Based on the ratio measurements of the full model, similar trend was observed for $\mu = 1$, which is closer to the neglected mobility

assumption (Figure 5.4). And to summarize the findings from the comparisons of spatiotemporal variation, we could say that the measurements on the regular system based on the Gillespie algorithm incorporating movement agreed with the measurements on the simplified systems back in the previous Sections "Temporal variation", "Spatial variation" and "Temporal over spatial variation": both spatial and temporal, and the ratio of variations were increasing with increasing contribution of the competition to the death rates. Based on the positive relationship of the ratio with δ, we expect that selection will favor faster dispersers as the death rates become more competition-dependent. Next, we will continue with the interpretation of the evolutionary outcomes based on the measured temporal and spatial variation of non-evolving equilibrium populations. As theoretical and empirical observations suggest, we will not focus on each type of variation independently, but mainly on the ratio of their comparison: temporal variation over spatial variation.

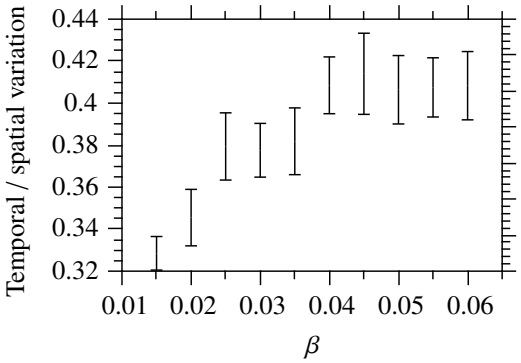

Figure 5.4: Ratio of temporal over spatial variation, of non-evolving equilibrium populations with $\mu = 1$, in respect to β under strong competition. Details for the method of spatiotemporal variation calculation can be found in Section "Measuring variation". The error bars denote the error of the ensemble mean. Parameters: $\kappa_\mu = 10^{-4}$, $\mu = 1$, $R = 0.1$, $r_{b0} = 1$, $r_{d0} = 0.1$, $\gamma = 0.06$, $N(0) = 1500$.

First, we will give an explanation, in terms of spatial and temporal variation, for the departure of the evolutionary trajectories from the minimum mobility end, for increasing δ (Figures 5.2 a and c, and 5.3 a). We saw that the first value at around which faster dispersal was selected, if starting from $\mu = 1$, must lie in the interval $\delta \in (0.5, 0.67)$ or else in $\beta \in (0.03, 0.04)$ (Figure 5.3 a). We suspect, according to theory, that a net increase in temporal in respect to spatial variation, $\bar{s}_t/\bar{s}_{sp}$, must have occurred for increasing δ in that interval. Indeed, the measured $\bar{s}_t/\bar{s}_{sp}$, for non-evolving populations of $\mu = 1$, was found to increase from below around 0.4 to above 0.4, exactly on that interval, i.e., $\beta \in (0.035, 0.04)$ (Figure 5.4). Thus, we assume from here on this Section, that a $\bar{s}_t/\bar{s}_{sp}$ value greater than 0.4 selects positively for faster dispersal. And as a remark, in this study a black box approach will be followed regarding the value of $\bar{s}_t/\bar{s}_{sp}$ above which faster dispersal is selected. Thus, we will not delve into the investigation of the reasons why this value triggers a redirection of selection, but instead we will consider it as a given fact. This postulation of the threshold $\bar{s}_t/\bar{s}_{sp}$ value of 0.4 will now be illustrated with a previously presented example of an evolutionary trajectory during which no departure was observed towards higher mobility (Figure 5.2 a). Upon reaching equilibrium, mutations were allowed to occur in the $\mu = 1$ and $\delta = 0$ population of lower $\bar{s}_t/\bar{s}_{sp}$. The population was at the minimum of the

specified mobility range, and thus the mutations changing the μ of the offspring were only those which were increasing μ. Under a regime which was not favoring faster dispersal ($\bar{s}_t/\bar{s}_{sp} < 0.4$), the growth of the more mobile mutants was limited, and the main bulk of the population, which was more adaptive under this spatially variable regime, had the lowest mobility allowed. Next, we will attempt to explain the rest of the presented examples of evolutionary outcomes, based mainly on the ratio $\bar{s}_t/\bar{s}_{sp}$.

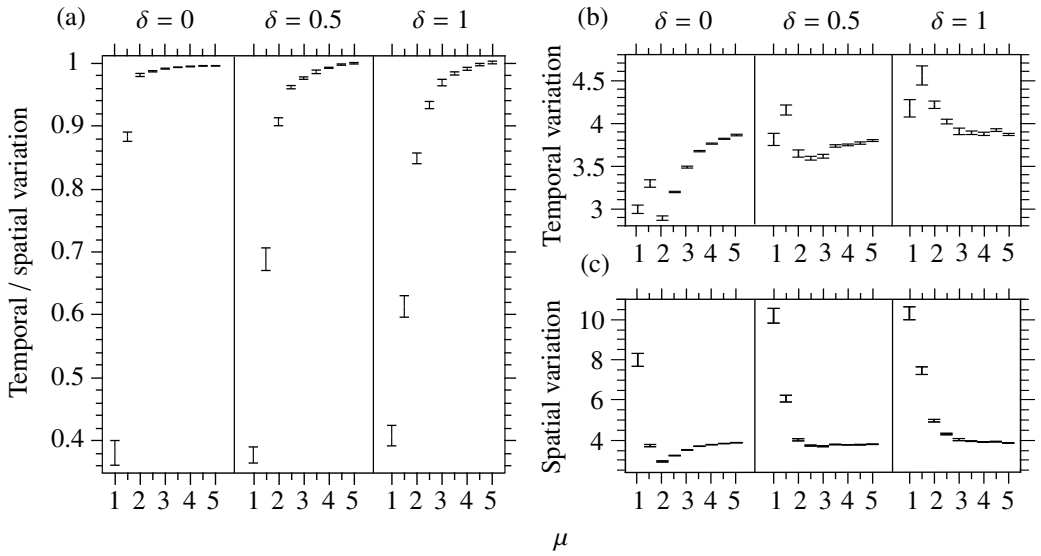

Figure 5.5: Temporal and spatial variation of non-evolving equilibrium populations in respect to μ and δ under strong competition. Details for the method of spatiotemporal variation calculation can be found in Section "Measuring variation". (a) ratio of temporal over spatial variation; (b) temporal variation; (c) spatial variation. The error bars denote the error of the ensemble mean. Parameters: $\kappa_\mu = 10^{-4}$, $R = 0.1$, $r_{b0} = 1$, $r_{d0} = 0.1$, $\gamma = 0.06$, $N(0) = 1500$.

We explained the $\delta = 0$ case, competition affecting only the birth rates, in the low mobility regime, and now we will continue with the $\delta = 1$ case of competition affecting only the death rates, again in the low mobility regime. In specific, the trajectory was starting with $\mu = 1$, and upon reaching equilibrium it was heading towards faster dispersal, rather slowly in the $\mu < 2$ range, and then faster in the $\mu > 2$ range (Figure 5.2 c). For maximum contribution of the competition to the death rates ($\beta = 0.06$, $\gamma = 0.06$, and thus $\delta = 1$), and lowest mobility ($\mu = 1$), $\bar{s}_t/\bar{s}_{sp} > 0.4$ (Figure 5.4), and thus faster dispersal is expected to be favored. More mobile mutants are then enjoying weaker competitive pressure than less mobile ones, and grow in numbers. The continuous production of mutations is mainly favored to the right of μ, and the μ distribution is expanding and getting flatter, with the fastest individuals having μ almost 2. The increase in higher mobility individuals in respect to less mobile ones, is expected to alter the ecological setting. For example, the ratio $\bar{s}_t/\bar{s}_{sp}$ of non-evolving equilibrium populations with $\mu = 1.5$ and $\delta = 1$ was estimated $\bar{s}_t/\bar{s}_{sp} = 0.614 \pm 0.018$ (Figure 5.5 a, for $\delta = 1$ and $\mu = 1.5$). Hence, we expect that $\bar{s}_t/\bar{s}_{sp}$ has increased in the example of our evolving population as well. Notice at this point, in Figure 5.5, that while spatial and temporal variation, as it has been already mentioned, do not follow a monotonous trend, the ratio $\bar{s}_t/\bar{s}_{sp}$ does, and this happens in all δ values con-

sidered there. This is crucial for the outcome of our example (the steepness of the monotonous increase will be adopted as an explanation of the evolutionary speed and directionality later on). Because of the monotonous increase of $\bar{s}_t/\bar{s}_{sp}$ with μ, a positive eco-evolutionary feedback loop is expected to take place: Being in a highly variable temporally environment (in respect to spatial variability always), faster dispersers are selected. As they increase in numbers because of the positive selection, they increase more the relative size of temporal in respect to spatial variation, which selects for even more mobile individuals. The whole eco-evolutionary process will lead the population to be composed by the fastest dispersers allowed. Still, though, we expect that due to the continuous, unavoidable insertion of new mutants, less mobile individuals will constantly be produced, creating a left tail to the extreme end mobility distribution. As a final note, the existence of a positive eco-evolutionary feedback could be given as the reason why intermediate mobility values will not be observed in this model under this setting. Selection is directed to an end, where favored mutants create an environment even more favorable for them. As long as there is not an opposing selective force, or a trade-off of some kind, no intermediate values will be observed as in Waddell et al. (2010). The distinguishing characteristic is that their model does not incorporate eco-evolutionary feedback. Temporal and spatial variation in their model are exclusively external forces, and thus they manage to shape mobility to intermediate values. In the present model, both kinds of variation are shaped by the individuals, which are then selected by their self-created environment.

When presenting the results of this Section, we distinguished two emerging trends: for a given contribution of competition to the death rates, δ, a higher mobility range selected stronger for higher mobility; and for a given mobility range, increasing δ selected stronger for higher mobility. Both of these trends could be understood in terms of the values and steepness of $\bar{s}_t/\bar{s}_{sp}$ in Figure 5.5 a. A $\bar{s}_t/\bar{s}_{sp} > 0.4$ would mean selection for higher mobility, and a larger $\bar{s}_t/\bar{s}_{sp}$ above the threshold would mean even stronger selection towards the highest mobility end. Evolutionary speed and directionality could be explained in terms of both absolute values and steepness: greater speed and directionality would be expected under simultaneously larger $\bar{s}_t/\bar{s}_{sp}$ values and higher steepness of $\bar{s}_t/\bar{s}_{sp}$ with μ. Regarding the first trend, the example trajectories we have been exposed to the shift in mobility selection with a change in the mobility range (Figure 5.2 a and b), and the more determined and rapid character of evolutionary convergence as the μ distribution had passed $\mu \approx 2$ (Figure 5.2 c), could be explained based on the aforementioned remarks. In the former example, by starting from $\mu = 2$, $\bar{s}_t/\bar{s}_{sp}$ was well above threshold (Figure 5.5 a, for $\delta = 0$); and in the latter, even though the steepness had decreased a little, $\bar{s}_t/\bar{s}_{sp}$ was larger in the $\mu > 2$ range (Figure 5.5 a, for $\delta = 1$). For the second trend, let us take a look at two examples. The first one, the departure of the evolutionary trajectory from the low mobility end, $\mu = 1$, when δ was larger (Figure 5.2 a and c), has been already explained. We based our explanation on the fact that the only thing which we were expecting to increase so that a redirection of selection would occur, would be an increase in $\bar{s}_t/\bar{s}_{sp}$. Indeed, because $\bar{s}_t/\bar{s}_{sp} > 0.4$ for $\delta = 1$, a shift in the selection occurred. The second example regards the thinner and more stable left tail of the distribution at the maximum mobility end, when δ was again larger (Figure 5.2 b and d). This could be explained by a comparison of the two δ cases in Figure 5.5 a, for $\delta = 0$ and $\delta = 1$ in the $\mu \in [2, 3]$ range. For $\delta = 0$, $\bar{s}_t/\bar{s}_{sp}$ has larger values and the change of the values with μ is smaller. The ecological setting has so large $\bar{s}_t/\bar{s}_{sp}$ that it is almost the same if it is occupied by individuals with $\mu = 2$, $\mu = 2.5$, or $\mu = 3$. This is denoted by the low steepness of $\bar{s}_t/\bar{s}_{sp}$ with μ. And it means that if we start with $\mu = 3$, lower mobility mutants receive weaker negative selection. As a consequence, the μ distribution would be expected to be more expanded, and less attached to the maximum mobility end. As this Section arrives to its end, let us follow the

temporal change in temporal and spatial variation of evolving populations. There, we will test if the interpretation from the non-evolving populations is in agreement with what the evolving ones show, and if there is additional insight offered by this different approach.

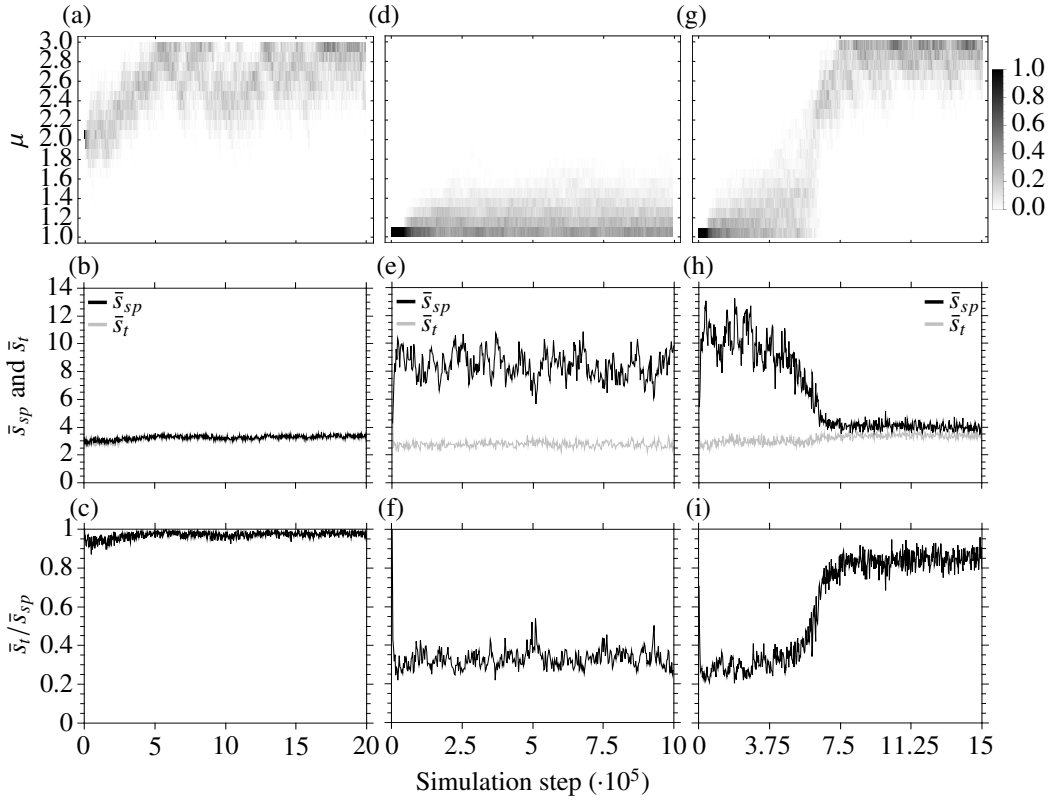

Figure 5.6: Temporal change in the distribution of μ and in the corresponding spatial and temporal variation ($\bar{s}_{sp}$ and $\bar{s}_t$, respectively) of evolving populations, under strong competition and various degrees of the competition's contribution to the death rates, δ. (a), (b) and (c) $\delta = 0$; (d), (e) and (f) $\delta = 0.5$; (g), (h) and (i) $\delta = 1$. The μ distributions are depicted vertically, where darker color, according to the legend, denotes higher relative frequency of μ in the bins. Mutations were allowed upon reaching equilibrium. The individuals' offspring were mutating their μ by a quantity drawn uniformly from the interval $(-0.05, 0.05)$. Details for the method of $\bar{s}_{sp}$ and $\bar{s}_t$ calculation can be found in Section "Measuring variation". Variation was calculated at every subsequent interval of 2500 simulation steps. Parameters: $\kappa_\mu = 10^{-4}$, $R = 0.1$, $r_{b0} = 1$, $r_{d0} = 0.1$, $\gamma = 0.06$, $N(0) = 1500$.

Let us take a look at the spatiotemporal variation's trajectories of three cases of evolving populations (Figure 5.6). All these cases should be familiar to the reader, since they have been examined previously in this Section. For the first column of Panels (Figure 5.6 a, b and c), for competition solely on the birth rates ($\delta = 0$) and initial $\mu = 2$, evolution headed towards higher mobility, and attached to the maximum mobility end, even though not so strongly. Both spatial and temporal variation were having almost the same values, their ratio was very close to

1. During the period of the distribution's shift to the right, the ratio of the variations increased. Thus, as the distribution was moving to the right, mainly temporal variation increased. And the same was happening to the other direction: For example, notice that during the large drop in the peak of the distribution around the middle of the simulation, the ratio decreased, and if we could focus we could see that this was due to a decrease in temporal variation. The values that the trajectories followed are in agreement with the respective measurements from the non-evolving populations (Figure 5.5). Thus, upon equilibrium and its subsequent beginning of mutations, the large $\bar{s}_t/\bar{s}_{sp}$ was selecting for higher mobility. The main ecological effect of this selection was an increase in the temporal variation of the environment, and a subsequent selection of even more mobile individuals. Notice, though, that in this highly variable temporally environment, individuals with mobility lower than the maximum are weakly selected, and there are large shifts in the mobility distribution.

In the second column of Panels (Figure 5.6 d, e and f), we have the case of $\delta = 0.5$ and initial $\mu = 1$. The value of δ is close enough before the value at which we located the redirection of selection from the lowest $\mu = 1$ to the highest μ (Figure 5.3 a). The distribution is stabilized, having the right tail due to mutations. Approximately, the two variations fluctuate below the values obtained from non-evolving populations (Figure 5.5 b and c, for $\delta = 0.5$ and $\mu = 1$), while their ratio fluctuates on around the similar level (Figure 5.5 a, for $\delta = 0.5$ and $\mu = 1$). Perhaps, the existence of larger μ mutants is the reason for this discrepancy. Noticeable are the larger fluctuations of the spatial variation. And if we forego to the next column, we will see that at $\delta = 1$ spatial variation in time fluctuates similarly. According to the patterns in non-evolving populations (Figure 5.5 a, b and c), it seems that no apparent difference is evident. The only thing that could be thought, and the only thing that for sure changes is δ. It has been noted (Hernández-García et al., in press), and possibly observed here (Figure 4.7 comparison between Panels), that the periodicity of the clusters is more irregular for larger δ. This fact, coupled with the higher temporal variation in larger δ, maybe is responsible for the larger size of the spatial variation's fluctuations.

Finally, in the third column (Figure 5.6 g, h and i), for $\delta = 1$, we have the departure of the evolutionary trajectory towards the highest of mobility. First, by comparing the second with the third column, we see that for $\delta = 1$, the spatial and temporal variation of the population at its initial mutational stages are relatively larger than the ones for $\delta = 0.5$, but the ratio seems similar. The most significant phenomenon observed is the decrease in spatial variation as mutations are starting to be produced after the population equilibrium, and this is followed by a net increase in the ratio $\bar{s}_t/\bar{s}_{sp}$. Notice that the ratio fluctuates below the threshold value we assumed, $\bar{s}_t/\bar{s}_{sp} \approx 0.4$. But again, the same applies and to its fluctuating value after the distribution had reached its new evolutionary stability (compare with Figure 5.5 a, for $\delta = 1$ and $\mu = 3$). All in all here, a rough visual inspection was offered. Of course, solid conclusions could be drawn from the statistical and theoretical analysis of the temporal dynamics of variation. Nevertheless, it was judged that the temporal dynamics of variation during evolution would be an interesting picture to inspect, even visually. We saw that, depending on the case, either spatial or temporal variation seems to lead the dynamics towards new evolutionary stability. On the other hand, someone could note that the eco-evolutionary dialogue that is at play continuously, should not allow us to determine a principal driver of the dynamics. Are spatial and temporal variation the drivers or the end results of dispersal evolution?

5.3. Weak competition

In this Section, we will consider weaker competition ($\gamma = 0.02$) in respect to the previous Section's stronger competition ($\gamma = 0.06$). The influence of the evolution of dispersal by the competition's contribution to the death rates will be investigated again for this weak competition setting. Initially, it will be investigated by observing the temporal change of individual mobility during simulations of evolution. And next, the simulations of evolution will be interpreted in terms of measured spatiotemporal variation of non-evolving and evolving populations.

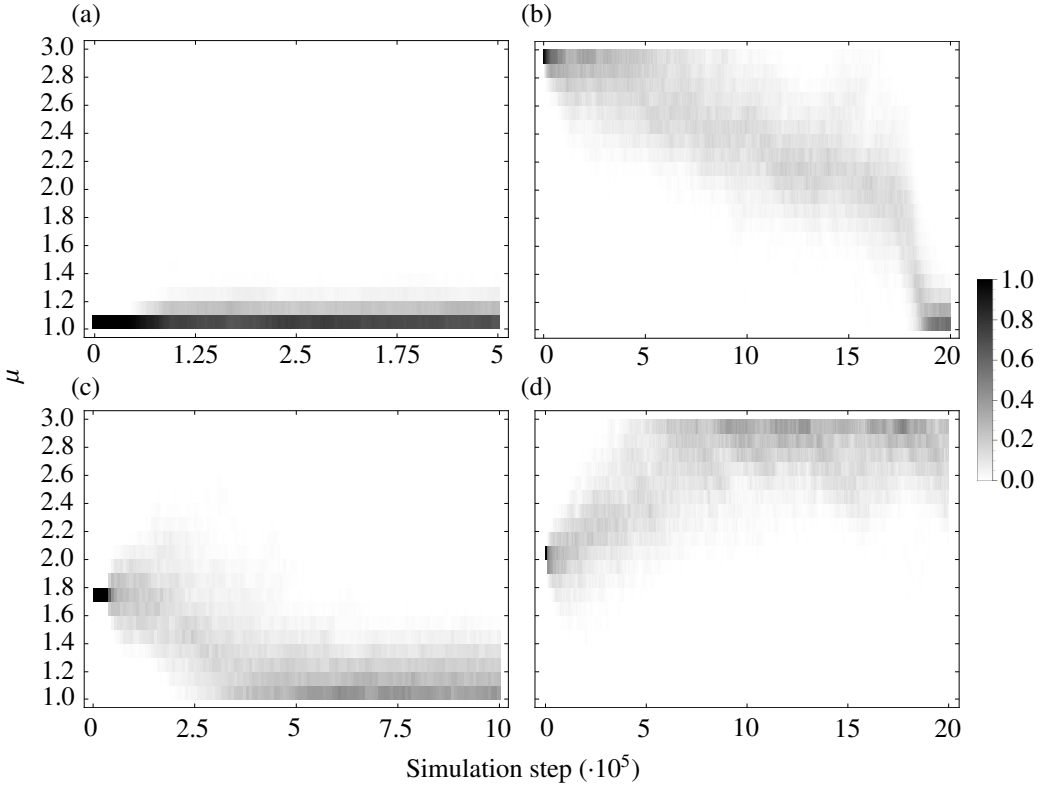

Figure 5.7: Temporal change in the distribution of μ during simulations of μ evolution under weak competition ($\gamma = 0.02$). The distributions are depicted vertically, where darker color, according to the legend, denotes higher relative frequency of μ in the bins. (a) and (b) $\delta = 0$, and simulation started with all individuals having $\mu = 1$ and $\mu = 3$, respectively; (c) and (d) $\delta = 1$, and simulation started with all individuals having $\mu = 1.75$ and $\mu = 2$, respectively. Mutations were allowed upon reaching equilibrium. The individuals' offspring were mutating their μ by a quantity drawn uniformly from the interval $(-0.05, 0.05)$. Parameters: $\kappa_\mu = 10^{-4}, R = 0.1$, $r_{b0} = 1$, $r_{d0} = 0.1$, $\gamma = 0.02, N(0) = 1500$.

For the competition affecting only the birth rates case, $\delta = 0$, we will follow the evolution of μ, starting from either of the two extremes of our predetermined range: $\mu \in [1, 3]$. Starting from $\mu = 1$, no net evolutionary change had been observed (Figure 5.7 a). If starting from the other extreme, from $\mu = 3$, the distribution was driven again to the lowest μ allowed (Figure 5.7

b). The evolving population needed relatively longer time to slowly descent in μ values, until its main bulk reached $\mu \approx 2$, and then it headed faster to the $\mu = 1$ end. Thus, in weaker competition ($\gamma = 0.02$) affecting only the birth rates ($\delta = 0$), slower dispersal was selected in both mobility regimes, for the parameter values considered.

Now, on the competition affecting only the death rates case, $\delta = 1$. A noticeable thing in the simulation of evolution of Figure 5.7 b, was the difference in the speed of evolutionary change between the $\mu > 2$ and the $\mu < 2$ ranges. Even though evolution seemed to have a clear directionality in either side of $\mu \approx 2$, the greater speed by which the population evolved in the $\mu < 2$ range could indicate a stronger selective regime for slower dispersal. Being better informed by this observation, we will follow simulations of evolution for $\delta = 1$ starting close to $\mu = 2$. If starting with all individuals having $\mu = 1.75$, the population was evolving towards the slowest dispersal again (Figure 5.7 c). If the initial $\mu = 2$, then evolution, instead of moving to lower mobility, approached and stayed on the maximum mobility end (Figure 5.7 d). These outcomes could strengthen our suspicions that the $\mu < 2$ promotes a different selective regime in respect to the $\mu > 2$ range, again here. Hence, in weaker competition ($\gamma = 0.02$) affecting only the death rates ($\delta = 1$), slower dispersal was selected by starting in a lower range of mobility, and faster dispersal was selected in a higher mobility range.

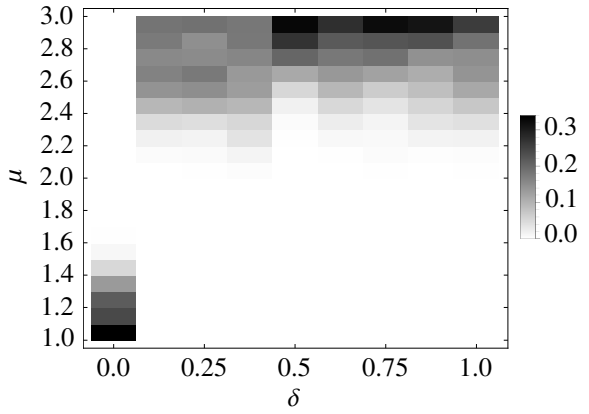

Figure 5.8: Evolutionary equilibrium distributions of movement parameter μ for various degrees of the competition's contribution to the death rates, δ, under weak competition γ, and starting from maximum mobility allowed. The distributions are depicted vertically, where darker color, according to the legend, denotes higher mean relative frequency of μ in the bins. For each δ, a single simulation of evolution was carried out, starting with $\mu = 3$, and mutations were allowed upon reaching equilibrium. Each rectangle is the temporal mean for a duration of $t = 100$, sampled every $t = 5$, after the distribution had reached a final, relatively unchanged state. The individuals' offspring were mutating their μ by a quantity drawn uniformly from the interval $(-0.05, 0.05)$. Parameters: $R = 0.1$, $r_{b0} = 1$, $r_{d0} = 0.1$, $\gamma = 0.02$, $N(0) = 1500$.

When competition was impacting only the birth rates, the evolutionary stable mobility was the lowest, even starting the simulations with maximum mobility (Figure 5.7 a and b). The evolutionary trajectory was passing, even slowly, the $\mu > 2$ range, towards lower mobility. But this changed for the $\mu > 2$ range, when competition was affecting only the death rates, $\delta = 1$. Then, the evolutionary trajectory was not moving to lower mobility, but higher mobility

was selected (Figure 5.7 d). We could take more, intermediate values of δ again here, and by starting each simulation of evolution from $\mu = 3$, we could identify a shift in the selection towards lower mobility in the $\mu > 2$ range. Figure 5.8 shows that the shift must be found in $\delta \in (0, 0.125)$, for $\gamma = 0.02$ considered here. Notice in Figure 5.8, in addition, that the first three evolutionary equilibrium distributions after the shift in the selection of mobility (i.e., for $\delta = 0.125,\ 0.25,\ 0.375$) have flatter peaks, still towards the maximum of mobility. Since the values in the distributions' bins were temporal averages of relative frequency, the broader peaks mean that the distributions either were broader during the simulation or they were moving occasionally to lower mobility. In either case, this could be an indication that, as δ increased, the selective force for higher mobility was getting stronger.

Again here, as in stronger competition, the same two trends were revealed. First, for a given contribution of competition to the death rates, δ, evolution in a lower mobility regime was attracted stronger to the lowest mobility. By this remark we could justify: the greater speed in evolution when the distribution was in the $\mu < 2$ range, for $\delta = 0$ (Figure 5.7 b); and the shift in selection between the two ranges, for $\delta = 1$ (Figure 5.7 c and d). Second, for a given mobility regime, increasing the competition's contribution to the death rates, lead to stronger selection for higher mobility. By this remark we could justify: the flatter distribution around the maximum mobility for decreasing δ, for the $\mu > 2$ mobility regime (Figure 5.8); the fatter right tail of the μ distribution for $\mu < 2$ (Figure 5.7 a and c); and the shift in mobility selection, from lower to higher mobility for $\mu > 2$ (Figure 5.7 b and d). Additionally, we spotted the same occurrence of the $\mu \approx 2$ acting as a border, separating two different evolutionary behaviors. As we noted previously, for larger δ, a force acting towards the selection of faster dispersal seemed to be at play. Thus, we could speculate that in the competition between clustering and this force, the latter won in the $\delta = 1$ and $\mu > 2$ setting. Having already acknowledged the inability of clustering to elucidate on the interpretation of these outcomes, we will turn directly to the explanations based on spatial and temporal variation. First, in this explanatory part, we will expose again the expectations and speculations appeared in Sections "Temporal variation". "Spatial variation" and "Temporal over spatial variation" to the measured spatial and temporal variation of non-evolving equilibrium populations.

Beginning with temporal variation, and regarding δ, in simulations of non-evolving populations at equilibrium, where mobility was also incorporated, generally the same positive relationship was observed as in Section "Temporal variation" (Figure 4.3 a, for weak competition $\gamma = 0.02$): for a given μ, temporal variation was increasing with δ. But for a given δ, temporal variation was following a characteristic pattern with μ (Figure 5.11 b): starting from $\mu = 1$, it was reaching a local maximum at $\mu \approx 1.25$, then decreasing until $\mu \approx 1.75$, and finally it was increasing again, until $\mu = 3$. Thus, another intriguing pattern arose when we included mobility, and the existence of the critical value of $\mu \approx 1.81$ for pattern formation may be at play again. Lastly, we speculated that increasing mobility may tend to alleviate high temporal fluctuations. Here we saw that generally temporal variation was increasing with μ (Figure 5.11 b), even though for increasing δ, and therefore for increasing temporal variation, the increase of temporal variation with μ was less profound. In conclusion, even without neglecting mobility, higher contribution to the death rates, δ, was coupled by higher temporal variation. And movement by its own had the effect of increasing temporal variation, even though its effect was weaker in temporally more variable environments because of increased contribution of competition to the death rates, δ.

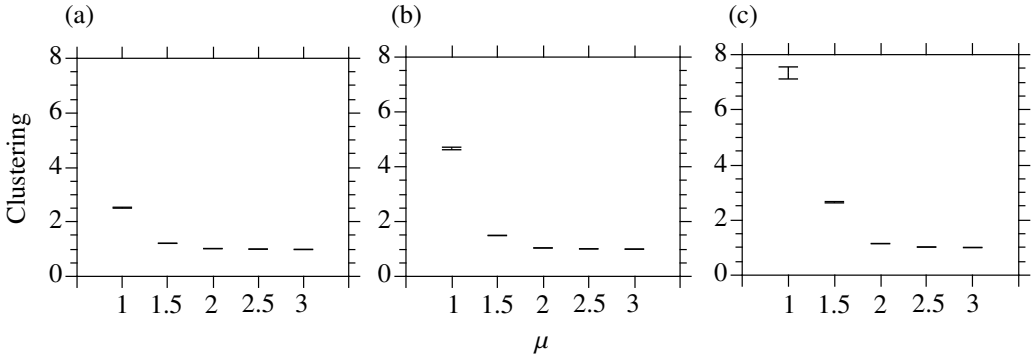

Figure 5.9: Clustering in respect to μ for three values of the competition's contribution to the death rates, δ, under weak competition γ. A uniform spatial configuration has a clustering value equal to 1. Details of the clustering's calculation method can be found in Section "Spatial variation". (a) $\delta = 0$; (b) $\delta = 0.125$; (c) $\delta = 1$. The error bars denote the error of the ensemble mean. Other, common-valued parameters: $\kappa_\mu = 10^{-4}$, $R = 0.1$, $r_{b0} = 1$, $r_{d0} = 0.1$, $\gamma = 0.02$, $N(0) = 1000$.

Concerning spatial variation, we speculated that clustering and spatial variation, in terms of N_R, should not be considered synonymous, according to their definitions. A comparison between Figure 5.9 a, and Figure 5.11 c, will reveal the difference. While clustering decreased monotonously (Figure 5.9 a), spatial variation decreased until $\mu = 1.75$, kept this lowest value until $\mu = 2$, and then increased again (Figure 5.11 c, in the leftmost Subpanel, for $\delta = 0$). For larger δ, the monotonous decrease of spatial variation resembles the one of clustering, but based on smaller δ, we could say that clustering is not the same as spatial variation. The same intriguing minimum of spatial variation located at $\mu = 1.75$ and $\mu = 2$ was found and here, and, as it was mentioned before, we will overlook it. On the other hand, we observed in Section "Spatial variation" that clustering and spatial variation was increasing with increasing δ (Figures 5.9, and 4.5 a, for $\gamma = 0.02$, respectively). But spatial variation was not found to increase as much as clustering with increasing δ, in the full model (compare Figures 5.9 and 5.11 c). Comparing the $\delta = 0$ with the $\delta = 1$ case, while spatial variation increased from around 21 to around 23 individuals, clustering increased from a value of around 2.5 to around 7.5, for $\mu = 1$. Again, the same explanation, based on the limited range of inter-cluster distance and the pattern periodicity, could be invoked for this behavior, as in Section "Strong competition".

Finally, regarding the ratio of temporal over spatial variation, in Section "Temporal over spatial variation" it was shown that it follows a positive relationship with the competition's contribution to the death rates (Figure 4.8 a, for $\gamma = 0.02$). Based on the ratio measurements of the full model, similar trend was observed for $\mu = 1$, which is closer to the neglected mobility assumption (Figure 5.11 a, comparison among δ, for $\mu = 1$). And to summarize the findings from the comparisons of spatiotemporal variation, we could say that the measurements on the regular system based on the Gillespie algorithm incorporating movement agreed with the measurements on the simplified systems back in Sections "Temporal variation", "Spatial variation" and "Temporal over spatial variation": both spatial and temporal, and the ratio of variations were increasing with increasing contribution of the competition to the death rates. Based on the positive relationship of the ratio with δ, we expect that selection will favor faster dispersers as the death rates become more competition-dependent, under weak competition as well. Next, we will

continue with the interpretation of the evolutionary outcomes based on the measured temporal and spatial variation of non-evolving equilibrium populations. Having already the experience of the explanatory way in terms of spatiotemporal variation and eco-evolutionary feedback, in this Section we will pass in less detail from an explanation of the evolutionary outcomes presented. Essentially, apart from the differences because of the different γ, which will be discussed in Section "Weak-strong competition comparison", the same qualitative behavior was exhibited under weak competition.

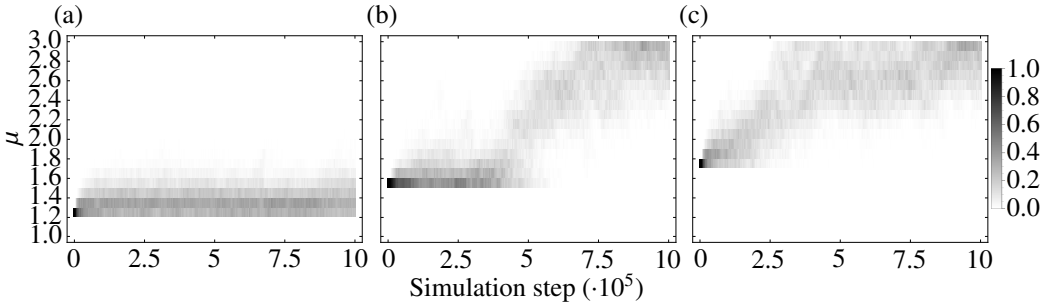

Figure 5.10: Temporal change in the distribution of μ during simulations of μ evolution under weak competition ($\gamma = 0.02$) affecting solely the death rates ($\delta = 1$). The distributions are depicted vertically, where darker color, according to the legend, denotes higher relative frequency of μ in the bins. The initial μ was also the lowest μ allowed: (a) $\mu = 1.25$; (b) $\mu = 1.5$; (c) $\mu = 1.75$. Mutations were allowed upon reaching equilibrium. The individuals' offspring were mutating their μ by a quantity drawn uniformly from the interval $(-0.05, 0.05)$. Parameters: $\kappa_\mu = 10^{-4}$, $R = 0.1$, $r_{b0} = 1$, $r_{d0} = 0.1$, $\gamma = 0.02$, $\delta = 1$, $N(0) = 1500$.

Let us begin, then, by the essential identification of the approximate value above which faster dispersal was selected. In this setting, no departure towards faster dispersal occurred if starting from $\mu = 1$, even for $\delta = 1$. First of all, notice that the maximum value of $\bar{s}_t/\bar{s}_{sp} \approx 0.27$ (Figure 5.11 a, for $\delta = 1$ and $\mu = 1$), which is much smaller that the above 0.4 value of the respective $\delta = 1$ case under stronger competition. The problem is that we cannot search quite precisely the threshold in larger $\bar{s}_t/\bar{s}_{sp}$, since the existence of mutations at lower mobility tends to drive the evolution to the lowest mobility. If we run evolutionary simulations, starting from, let us say, $\mu = 1.25$, the lower mobility mutants in such low values of $\bar{s}_t/\bar{s}_{sp}$ will take over the population by forming clusters, and thus hide the threshold $\bar{s}_t/\bar{s}_{sp}$. In the stronger competition setting, we were lucky because the minimum value of $\mu = 1$ we chose was the first in the $\delta = 1$ case to have $\bar{s}_t/\bar{s}_{sp} > 0.4$. So, the trick now is to manipulate the minimum of the mobility range, so that no mutations with lower mobility would interfere with the search of the first value of ratio leading to departure towards the highest mobility. Thus, simulations of evolution were run with an initial $\mu = 1.25$, 1.5, 1.75 and 2, for $\delta = 1$. The lowest μ allowed was the same μ by which each simulation was starting. By this procedure, the first initial μ at which a redirection of selection occurred was $\mu = 1.5$ (Figure 5.10). Notice that when starting from $\mu = 1.75$ with $\delta = 1$ and minimum $\mu = 1$, evolution was driven to the lowest mobility (Figure 5.7 c); while for the same setting except that minimum $\mu = 1.75$, evolution was driven to the highest mobility (Figure 5.10 c). This could be explained by the aforementioned argument, that mutants with $\mu < 1.75$ bring greater ecological change towards lower mobility than higher mobility mutants do for higher mobility (Figure 5.11 a, for $\delta = 1$ and $\mu \in [1.5, 2]$). We are not in a position in

the present study to draw safe conclusions regarding the fact, or coincidence, that for $\mu = 1.5$ we have the first value of the ratio above 0.4, again like in strong competition (see Figure 5.11 a, for $\delta = 1$ and $\mu = 1.5$). Nevertheless, here we will care only about the value alone, and not for any relevance it may have for the evolutionary dynamics of the redirection from slower to faster dispersal, given the general setting of the model. As a double check, the same procedure was tried for $\delta = 0.125$. And again there, by increasing the initial μ, and the minimum μ allowed in consequence, the first μ at which the evolution headed to the highest mobility was $\mu = 1.5$, the first one with $\bar{s}_t/\bar{s}_{sp} > 0.4$, for $\delta = 0.125$. Hence, now we are in a position to justify the absence of redirection of selection for $\delta = 1$, while on contrast it occurred under stronger competition. Simply, the resident, equilibrium population with $\mu = 1$ creates an environment with $\bar{s}_t/\bar{s}_{sp} < 0.4$, so that faster dispersal is negatively selected. The created mutants are selected against, and their numbers remain only because of the generous and continuous production of mutations.

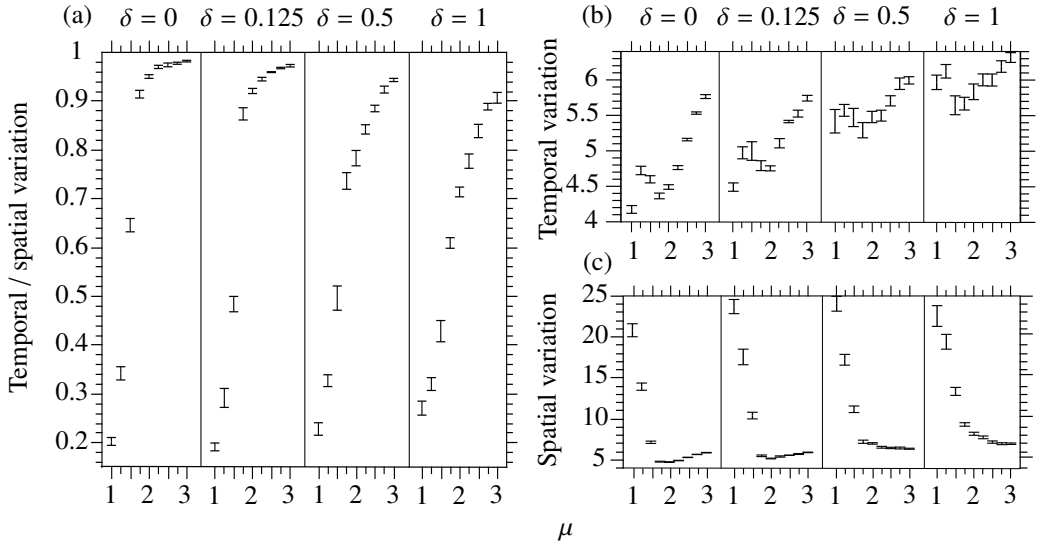

Figure 5.11: Temporal and spatial variation of non-evolving equilibrium populations in respect to μ and δ under weak competition. Details for the method of the spatiotemporal variation's calculation can be found in Section "Measuring variation". (a) ratio of temporal over spatial variation; (b) temporal variation; (c) spatial variation. The error bars denote the error of the ensemble mean. Parameters: $R = 0.1$, $r_{b0} = 1$, $r_{d0} = 0.1$, $\gamma = 0.02$, $N(0) = 1500$.

Before proceeding with explanations, we have to outline the relevance that mutations have for the evolutionary outcomes. Given the way and the size of the mutational change as it was implemented here, the spread of the μ distributions seems to have a maximum and minimum μ of around 0.5 larger and smaller than the central tendency of the distributions, if any. This is apparent when mutations are starting after the population had reached equilibrium, and before evolution starts to shape the distribution. For an example, look at Figure 5.7 c, where you can see that while the main bulk is at the initial value of $\mu = 1.75$, after almost $2 \cdot 10^5$ steps, the distribution has spread at around $\mu \in (1.3, 2.2)$. For the trajectory that started at $\mu = 1.75$ for $\delta = 1$ (Figure 5.7 c), we would expect that it will tend to faster dispersal, due to its high enough $\bar{s}_t/\bar{s}_{sp}$ (Figure 5.11 a, for $\delta = 1$ and $\mu = 1.75$). The reason for which this did not happen can

be derived from Figure 5.11 a. In this setting, faster dispersal is expected to be selected, and upon mutations the faster mutants are favored. But, two facts seem to constrain the growth of the more mobile individuals: the $\bar{s}_t/\bar{s}_{sp}$ is not that large, and the impact of lower mobility mutants on the ecological setting is greater. The asymmetry of the impact is inspired by the fact that by decreasing μ, the drop in $\bar{s}_t/\bar{s}_{sp}$ is greater than the increase in $\bar{s}_t/\bar{s}_{sp}$ by increasing μ (Figure 5.11 a, for $\delta = 1$ and $\mu \in [1.25, 2.25]$). That could be the reason for the final positive selection of the less mobile individuals. They alter the environment more towards their needs (the minimum of the distribution, in Figure 5.7 c, is reaching almost $\mu = 1.3$, which means cluster formation), and then they are selected positively because of that.

In essence, the shape of $\bar{s}_t/\bar{s}_{sp}$ with μ, in Figure 5.11 a, is similar to the respective-one of stronger competition (Figure 5.5 a). Thus, similar evolutionary outcomes were produced, and the explanation of stronger or weaker selection in respect to the mobility range and δ will not take place again. Hereon, we will be limited only to the interpretation of the interesting trajectory of $\delta = 0$, starting with $\mu = 3$ (Figure 5.7 b). The initial population had a very high $\bar{s}_t/\bar{s}_{sp}$, according to the measure on non-evolving populations (Figure 5.11 a, for $\delta = 0$ and $\mu = 3$). That is, the selection was strong towards faster dispersal. But, the change in $\bar{s}_t/\bar{s}_{sp}$ as μ decreases is relatively small. In fact, adjacent values have overlapping errors of the mean, until $\mu = 2$. This, in consequence, means weak negative selection of the lower mobility mutants until $\mu = 2$. The peak of the distribution drops, and it becomes flatter. The main volume of the distribution wanders in the $\mu \in (2, 3)$ range. Already because of the weak selection, the $\bar{s}_t/\bar{s}_{sp}$ is expected to drop, even a little, according to Figure 5.11 a. When the main bulk of the distribution happens to move close to $\mu = 2$, this means that a respected number of lower mobility mutants will be produced. Because of the fast production of mutations, the lowest mobility mutants can have $\mu \approx 1.5$. And if their numbers are adequately large, they can decrease dramatically the $\bar{s}_t/\bar{s}_{sp}$ setting. This is apparent from the rapid decrease in $\bar{s}_t/\bar{s}_{sp}$ for decreasing μ below 2 (Figure 5.11 a, for $\delta = 0$ and $\mu =< 2$). The rest of the story is known: the positive feedback loop gets stronger because of the steep slope in $\bar{s}_t/\bar{s}_{sp}$, and the population attaches to the lowest mobility rapidly.

Let us now see if the measurements of variation across time and during evolution agree with the previous interpretative attempts. In the first column of Panels (Figure 5.12 a, b and c), a trajectory from the setting we considered last is depicted (competition only in the birth rates, $\delta = 0$, and initial $\mu = 3$ under weak competition). As it was described based on Figure 5.11 a, the wandering of the distribution in the $\mu \in (2, 3)$ range was followed by a decrease in $\bar{s}_t/\bar{s}_{sp}$. Notice that at the times the distribution moves closer to $\mu = 2$, $\bar{s}_t/\bar{s}_{sp}$ drops more, because of a simultaneous increase in spatial and a decrease in temporal variation. Because of the lowered $\bar{s}_t/\bar{s}_{sp}$, lower mobility mutants are not so negatively selected. The accumulation of slower dispersers leads mainly to a faster decrease in temporal variation, and at some point the fast shift is realized by a vast increase in spatial heterogeneity, mainly due to the formation of clusters, and a decrease in temporal variation. In the second column of Panels (Figure 5.12 d, e and f), we are in $\delta = 0.125$, the first value that no departure from $\mu = 3$ was observed in this Section (Figure 5.8). During the full expansion of the distribution because of the mutations, a slight decrease in $\bar{s}_t/\bar{s}_{sp}$ can be observed, mainly due to a decrease in temporal variation. Finally, for even increased contribution of competition to the death rates, $\delta = 1$, and by starting with $\mu = 2$ (third column of Panels in Figure 5.12 g, h and i), evolution headed towards the fastest dispersal. The path to the maximum of the mobility range was accompanied by a decrease in spatial and an increase in temporal variation. Notice that, even though $\bar{s}_t/\bar{s}_{sp}$ is smaller in the third column than in the second, the distribution at the third column after reaching the maximum is little more peaky and concentrated to the extreme. The reason cannot be derived by this plot,

but we saw that it could be explained because of the steeper decrease in $\bar{s}_t/\bar{s}_{sp}$ with decreasing μ, so that slower dispersers are stronger selected negatively (Figure 5.11 a, comparison between $\delta = 0.125$ and $\delta = 0.1$, for $\mu = 3$).

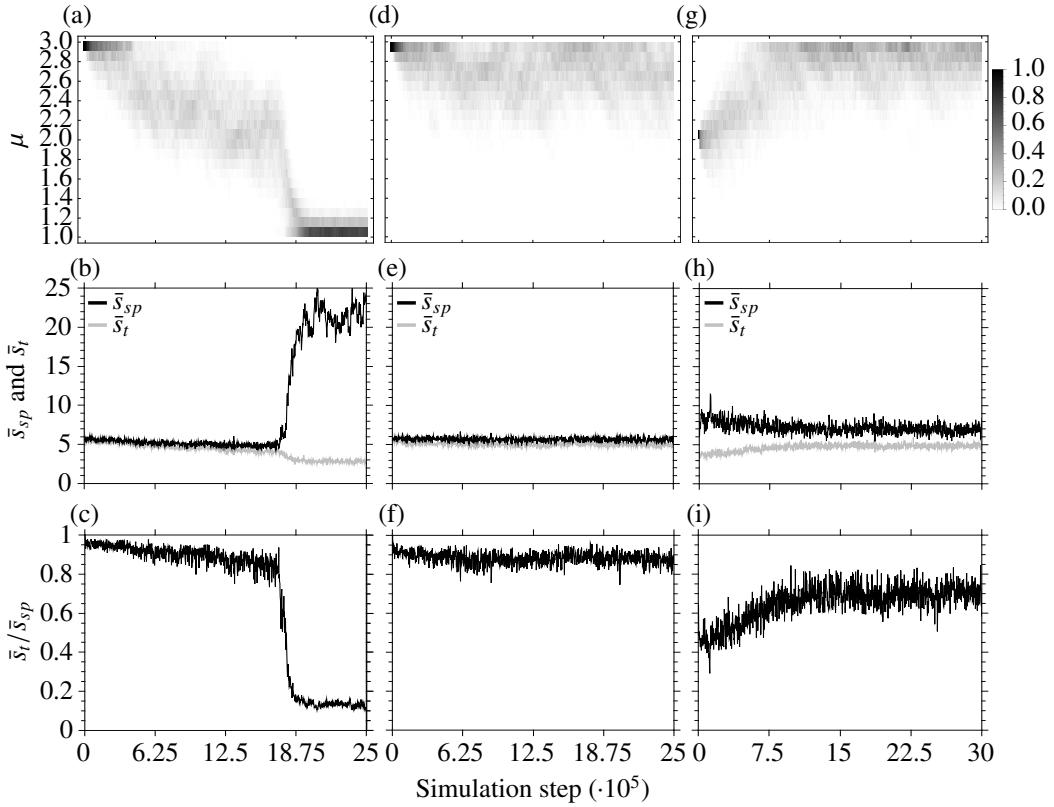

Figure 5.12: Temporal change in the distribution of μ and in the corresponding spatial and temporal variation ($\bar{s}_{sp}$ and $\bar{s}_t$, respectively) of evolving populations under weak competition, and for three levels of the competition's contribution to the death rates. (a), (b) and (c) $\delta = 0$; (d), (e) and (f) $\delta = 0.125$; (g), (h) and (i) $\delta = 1$. The μ distributions are depicted vertically, where darker color, according to the legend, denotes higher relative frequency of μ in the bins. Mutations were allowed upon reaching equilibrium. The individuals' offspring were mutating their μ by a quantity drawn uniformly from the interval $(-0.05, 0.05)$. Details for the method of $\bar{s}_{sp}$ and $\bar{s}_t$ calculation can be found in Section "Measuring variation". Variation was calculated at every subsequent interval of 2500 simulation steps. Parameters: $\kappa_\mu = 10^{-4}$, $R = 0.1$, $r_{b0} = 1$, $r_{d0} = 0.1$, $\gamma = 0.02$, $N(0) = 1500$.

5.4. Weak-strong competition comparison

In the last two Sections ("Strong competition" and "Weak competition"), we investigated the effect of the competition's contribution to the death rates under strong ($\gamma = 0.06$) and weak ($\gamma = 0.02$) competition. In this Section, we will take a look at the effect of competition intensity, γ. Initially, we will compare the findings from the simplified attempts in Sections "Temporal variation", "Spatial variation" and "Temporal over spatial variation", with the respective measures of

the full model with the Gillespie algorithm. Next, an interpretation of the evolutionary outcomes of Sections "Strong competition" and "Weak competition" will be attempted in respect to the effect of γ on the measured ratio of spatiotemporal variation of non-evolving populations with the full model. For the latter, we will focus on two pairs of Figures which were the central focus of this discussion (Figures 5.7 and 5.2, and Figures 5.11 and 5.5). These pairs will offer their suggestions and indications on different levels, so to have a more complete picture. Of course, each pair of equivalent Figures, is consisted by a weak and a strong competition counterpart.

Regarding temporal variation, Section "Temporal variation" showed that it must have a negative relationship with competition intensity γ (Figure 4.3 b). This relationship was confirmed by the measured temporal variation of non-evolving populations by the full model (comparison between each Subpanel of Figure 5.11 b, with its respective in Figure 5.5 b): in all considered degrees of the competition's contribution to the death rates, δ, temporal variation was lower at the stronger competition ($\gamma = 0.06$) setting. About spatial variation, again a negative relationship with competition intensity was identified (Figure 4.5 b). And the measured spatial variation of the full model was supporting this claim as well (comparison between each Subpanel of Figure 5.11 c, with its respective in Figure 5.5 c). Lastly, concerning the ratio of temporal over spatial variation, from the simplifications in Section "Temporal over spatial variation" it was found to increase with increasing competition intensity γ (Figure 4.8 b). And the same behavior was observed from the full model, especially for lower values of μ (comparison between each Subpanel of Figure 5.11 a, with its respective in Figure 5.5 a, but notice that in Figure 5.11 a, narrower μ range is considered).

Let us continue now with the comparison of evolutionary outcomes, with the pair of Figures 5.7 and 5.2, which will offer its indications in a rather phenomenological way. If you compare each Panel with its equivalent, the same trend arises: stronger competition tends to relax the selection for slower dispersal, or, equivalently, tends to enforce the selection for faster dispersal. Figures 5.7 a, and 5.2 a: the stronger competition counterpart has fatter right tail. Figures 5.7 b, and 5.2 b: on weaker competition the trajectory was heading to the lowest mobility, while in stronger competition was heading to the opposite direction. Figures 5.7 c, and 5.2 c: convergence to lower mobility for the weak competition, departure towards higher mobility under stronger competition. Figures 5.7 d, and 5.2 d: slow trajectory towards higher mobility, and fatter left tail as soon as it arrived to the extreme, under weaker competition; while rapid evolution and more peaked distribution to the fastest dispersal in the stronger competition setting. Thus, from this approach we could conclude that stronger competition, γ, increases the tendency for faster dispersal selection.

Now, let us turn to the pair of Figures 5.11 and 5.5, which provides indirect indications in a lower level, based on measurements made in equilibrium non-evolving populations. Since, according to all the considerations we, and the literature, have acquired until now, the ratio $\bar{s}_t/\bar{s}_{sp}$ is the crucial measure for the selection of dispersal, we will focus only on Figures 5.11 a, and 5.5 a. For $\delta = 0$: larger value on lowest mobility, and larger values with steeper slope on the higher mobility range, under stronger competition (Figure 5.5 a). For $\delta = 0.5$ and 1: qualitatively similar as in the $\delta = 0$ case. Thus, with this comparison we have an explanation, in terms of the opposition between temporal and spatial variation, for the patterns observed in the previous pair's comparison. How the shape and size of the relation of the ratio $\bar{s}_t/\bar{s}_{sp}$ with μ affect the selection of dispersal, has been already accounted in the last two Sections. The general conclusion, confirming the phenomenologically-based remarks of the previous comparison, is that stronger competition alters the ratio's $\bar{s}_t/\bar{s}_{sp}$ form of relation with mobility, such that selection of faster dispersal is encouraged.

6. Concluding remarks

This study confirmed from a different modeling perspective, in which spatial and temporal variation were not imposed explicitly or externally, the importance of the opposition between temporal and spatial variation for the evolution of mobility. In specific, the basic conclusions and contributions of the thesis were the following:

- Under this model's setting, the main effect of increasing the value of the Lévy index μ was an increase in mobility, and hence the evolution of dispersal was tracked by the evolutionary changing μ.
- Another component of temporal variation was recognized and judged appropriate for pursuing the goals of this study: the temporal variation in the neighborhood density due to demographic/movement events.
- Based on model simplifications, it was identified that faster dispersal should be favored under harsher survival conditions, i.e., under higher competition intensity or higher degree of the deaths being affected by competition.
- The method by which spatiotemporal variation was measured in the complete model, and the adoption of the eco-evolutionary point of view, were satisfactory means for explaining the evolutionary behaviors in the simulations of evolution.
- Under similar parameter values, the pairwise competition results of Heinsalu et al. (2013), concerning the superiority of species which form narrower clusters, were reproduced with this study's eco-evolutionary setting of simulating evolution.
- The simulations of evolution under the complete model confirmed that higher competition intensity, or larger impact of competition to the deaths, lead to selection for faster dispersal, because of increased temporal in respect to spatial variation.

After outlining what this study was about, let us list here what this study was not, and what it could be. First, it is acknowledged that we considered a tiny part of the parameter space. This study, lacking considerably a rigorous, quantitative character, could be better perceived as an exploratory, qualitative attempt to elucidate parts of the evolution of dispersal with this model. Additionally, it is acknowledged that this model is not to give definite answers to any of the open questions out there. The competition kernel was discrete, the individuals totally blind without sensing any gradient, reproduction was asexual, individuals could exist on the same spot, and movement did not impose any cost. Still, the insight gained could be illuminating for the real processes out there. Some questions and future perspectives could be listed: We came upon some intriguing patterns, that would be very interesting to study in detail. For example, why spatial variation was reaching its minimum in $\mu \approx 2$ and then increased for higher μ? Additionally, we did not consider the evolution of movement types, but only mobility in loose terms. It would be interesting to fix diffusivity so that we could follow only the evolution of movement types, from ballistic to Lévy to Brownian movement. Moreover, interesting would be the derivation of analytical expressions for spatial and temporal variation, in terms of demographic or movement parameters. We should not forget, as well, the intriguing threshold value of $\bar{s}_t/\bar{s}_{sp}$ above which faster dispersal was found to be selected. Was it a coincidence, or does it have an analytic basis? Finally, under the promising eco-evolutionary framework, it would be an interesting challenge to work analytically on the evolution of dispersal in this model, under the adaptive dynamics scheme.

7. Acknowledgements

Even though I was using first plural all over this text, here I would like in singular to thank the two senior scientists Emilio Hernández-García and Cristóbal López of the Institute for Cross-Disciplinary Physics and Complex Systems, IFISC (CSIC-UIB). It was a great pleasure to be supervised by you two. And I want to thank you once more for taking the effort to keep up such a rapid and vivid communication during the 2 months I was abroad. Additionally, my gratitude goes to Rubén Tolosa and Antònia Tugores, computer technicians in IFISC, for showing how to work on the 'Salmunia' computer. Finally, I would like to thank Dimitra Georgopoulou for the fruitful discussions we had during the whole course of the thesis; and Panagioti Kavakopoulo for the discussions, and for helping me to find a tiny bug in the bugs.

8. References

M. L. Baskett, J. S. Weitz, and S. A. Levin. The evolution of dispersal in reserve networks. *American Naturalist*, 170(1): 59–78, 2007.

S. P. Carroll, A. P. Hendry, D. N. Reznick, and C. W. Fox. Evolution on ecological time-scales. *Functional Ecology*, 21 (3):387–393, 2007.

M. L. Cody and J. M. Overton. Short-term evolution of reduced dispersal in island plant populations. *Journal of Ecology*, 84(1):53–61, 1996.

U. Dieckmann, B. O'Hara, and W. Weisser. The evolutionary ecology of dispersal. *Trends in Ecology & Evolution*, 14 (3):88–90, 1999.

J. Dockery, V. Hutson, K. Mischaikow, and M. Pernarowski. The evolution of slow dispersal rates: a reaction diffusion model. *Journal of Mathematical Biology*, 37(1):61–83, 1998.

R. P. Duncan, A. G. Boyer, and T. M. Blackburn. Magnitude and variation of prehistoric bird extinctions in the Pacific. *Proceedings of the National Academy of Sciences of the United States of America*, 110(16):6436–6441, 2013.

A. Hastings. Can spatial variation alone lead to selection for dispersal? *Theoretical Population Biology*, 24(3):244–251, 1983.

C. Hawkes. Linking movement behaviour, dispersal and population processes: is individual variation a key? *Journal of Animal Ecology*, 78(5):894–906, 2009.

E. Heinsalu, E. Hernández-García, and C. López. Competitive Brownian and Lévy walkers. *Physical Review E*, 85(4), 2012.

E. Heinsalu, E. Hernández-García, and C. López. Clustering determines who survives for competing Brownian and Lévy walkers. *Physical Review Letters*, 110(25), 2013.

E. Hernández-García and C. López. Clustering, advection, and patterns in a model of population dynamics with neighborhood-dependent rates. *Physical Review E*, 70(1):11, 2004.

E. Hernández-García, E. Heinsalu, and C. López. Spatial patterns of competing random walkers. *Ecological Complexity*, in press.

V. Hutson, K. Mischaikow, and P. Polacik. The evolution of dispersal rates in a heterogeneous time-periodic environment. *Journal of Mathematical Biology*, 43(6):501–533, 2001.

V. Hutson, S. Martinez, K. Mischaikow, and G. T. Vickers. The evolution of dispersal. *Journal of Mathematical Biology*, 47(6):483–517, 2003.

M. B. Kennel. KDTREE 2: Fortran 95 and C++ software to efficiently search for near neighbors in a multi-dimensional Euclidean space. *arXiv:physics/0408067v2 [physics.data-an]*, 2014.

D. A. Kessler and L. M. Sander. Fluctuations and dispersal rates in population dynamics. *Physical Review E*, 80(4):4, 2009.

C. Loehle. Challenges of ecological complexity. *Ecological Complexity*, 1(1):3–6, 2004.

S. McIntyre, S. Lavorel, and R. M. Tremont. Plant life-history attributes - their relationship to disturbance responses in herbaceous vegetation. *Journal of Ecology*, 83(1):31–44, 1995.

B. K. McNab. Energy conservation and the evolution of flightlessness in birds. *American Naturalist*, 144(4):628–642, 1994.

O. Ronce. *How does it feel to be like a rolling stone? Ten questions about dispersal evolution*, volume 38 of *Annual Review of Ecology Evolution and Systematics*, pages 231–253. Annual Reviews, Palo Alto, 2007.

O. Ronce and I. Olivieri. *Life history evolution in metapopulations*, chapter in *Ecology, Genetics, and Evolution of Metapopulations*, I. Hanski, and O. E. Gaggiotti (eds.), pages 227–258. Elsevier Academic Press, Amsterdam, 2004.

M. Saastamoinen. Heritability of dispersal rate and other life history traits in the Glanville fritillary butterfly. *Heredity*, 100(1):39–46, 2008.

O. Tange. GNU Parallel - the command-line power tool. *The USENIX Magazine*, 36(1):42–47, 2011.

J. N. Waddell, L. M. Sander, and C. R. Doering. Demographic stochasticity versus spatial variation in the competition between fast and slow dispersers. *Theoretical Population Biology*, 77(4):279–286, 2010.